



University of Tennessee, Knoxville
**Trace: Tennessee Research and Creative
Exchange**

Masters Theses

Graduate School

5-2006

Novel Materials Used in Hydrogen Energy Economy

Hongliang Zhou

University of Tennessee - Knoxville

Recommended Citation

Zhou, Hongliang, "Novel Materials Used in Hydrogen Energy Economy. " Master's Thesis, University of Tennessee, 2006.
https://trace.tennessee.edu/utk_gradthes/1849

This Thesis is brought to you for free and open access by the Graduate School at Trace: Tennessee Research and Creative Exchange. It has been accepted for inclusion in Masters Theses by an authorized administrator of Trace: Tennessee Research and Creative Exchange. For more information, please contact trace@utk.edu.

To the Graduate Council:

I am submitting herewith a thesis written by Hongliang Zhou entitled "Novel Materials Used in Hydrogen Energy Economy." I have examined the final electronic copy of this thesis for form and content and recommend that it be accepted in partial fulfillment of the requirements for the degree of Master of Science, with a major in Chemistry.

Jimmy W. Mays, Major Professor

We have read this thesis and recommend its acceptance:

Bin Hu, X. Peter Zhang

Accepted for the Council:

Dixie L. Thompson

Vice Provost and Dean of the Graduate School

(Original signatures are on file with official student records.)

To the Graduate Council:

I am submitting herewith a thesis written by Hongliang Zhou entitled “Novel Materials Used in Hydrogen Energy Economy.” I have examined the final electronic copy of this thesis for form and content and recommend that it be accepted in partial fulfillment of the requirements for the degree of Master of Science, with a major in Chemistry.

Jimmy W. Mays

Major Professor

We have read this thesis
and recommend its acceptance:

Bin Hu

X. Peter Zhang

Accepted for the Council:

Anne Mayhew

Vice Chancellor and Dean of Graduate Studies

(Original signatures are on file with official student records.)

**NOVEL MATERIALS USED IN
HYDROGEN ENERGY ECONOMY**

A Thesis
Presented for the
Master's of Science
Degree
The University of Tennessee, Knoxville

Hongliang Zhou
May, 2006

Copyright © 2006 by Hongliang Zhou
All rights reserved.

DEDICATION

This dissertation is dedicated to my great parents, Ruwen Zhou and Xiancui Ye. It is also dedicated to my former advisor, Prof. Y.Q. Jia, and all those friends who help, encourage, and inspire me on the way to my goal.

ACKNOWLEDGEMENTS

I wish to thank all those who helped me to complete my Master of Science degree. I would like to thank my principle advisor: Prof. Jimmy W. Mays for his great guidance and effort in make me familiar with materials used in hydrogen energy economy. I would like to thank Dr. Tianzi Huang for his kind help and support through the research process. I would like to thank both Dr. Bin Hu and Dr. X. Peter Zhang for serving on my committee. I would also like to thank everybody in Prof. Mays's group for the help and happy time of years.

Finally, I would like to thank my family and friends, whose suggestions and encouragement made this work possible.

ABSTRACT

The purpose of this study was to do some efforts in developing some novel polymer materials which could have the potential use in hydrogen pipelines and PEM fuel cell.

In the project of developing hydrogen pipelines, sulfonated PET, sulfonated PET/Clay and PET/Clay were produced by the method of solvent-mixing. Characterizations with TEM, SAXS were made to determine the exfoliation degree of nanocomposites. TGA was carried out to measure the thermal stability, and hydrogen permeability was also taken in order to measure the H₂ gas barrier performance. It was found that the addition of clay into S-PET or PET could decrease the hydrogen permeability in polymer nanocomposites.

In the other project of polymer electrolyte membrane in fuel cell, our research objective is to synthesize novel polymer electrolyte membrane (PEM) based on poly(1,3-cyclohexadiene) (PCHD) with outstanding potential for use in methanol fuel cells at temperatures well above 100 °C. After the consecutive crosslinking, aromatization and sulfonation reactions, or the consecutive crosslinking and sulfonation reactions, some novel PEM materials based on PCHD were synthesized. And a series of characterizations including FT-IR, elemental analysis, water-uptake, scanning electron microscopy (SEM), thermo gravimetric analysis (TGA), and proton conductivity were carried out.

TABLE OF CONTENTS

Chapter 1 INTRODUCTION.....	1
Chapter 2 RESEARCH BACKGROUND.....	2
2.1 Hydrogen Economy	2
2.1.1 What is the hydrogen economy?	2
2.1.2 Four parts of hydrogen economy.....	3
2.1.2.1 Hydrogen production.....	4
2.1.2.1.1 Production of hydrogen from fossil fuels.....	4
2.1.2.1.2 Production of hydrogen from water.....	6
2.1.2.1.3 Production of hydrogen from biomass.....	7
2.1.2.2 Hydrogen storage.....	8
2.1.2.3 Hydrogen delivery.....	9
2.1.2.4 Hydrogen utility.....	10
2.2 Hydrogen Pipeline.....	12
2.2.1 Advantages of hydrogen pipeline	13
2.2.2 Challenges of hydrogen pipeline	14
2.3 Fuel Cells (PEM Fuel Cells)	15
2.3.1 What is the fuel cell?	15

2.3.2 Types of fuel cells.....	17
2.3.2.1 Polymer electrolyte membrane fuel cells.....	17
2.3.2.2 Phosphoric acid fuel cells.....	20
2.3.2.3 Solid oxide fuel cells.....	20
2.3.2.4 Molten carbonate fuel cells.....	21
2.3.3 Applications of fuel cells.....	21
2.3.4 Future of fuel cells.....	22
 Chapter 3 NOVEL MATERIALS USED IN HYDROGEN PIPELINES...	23
3.1 Overview.....	23
3.2 Experiments.....	26
3.2.1 Materials.....	26
3.2.2 The synthesis of sulfonated PET	27
3.2.3 Preparation of PET/clay nanocomposites via solution mixing.....	28
3.2.4 Preparation of sulfonated PET/clay nanocomposites via solution mixing.....	28
3.2.5 Preparation of PET/clay nanocomposites via melt mixing.....	29
3.2.6 Material processing.....	30
3.2.7 Characterization	30
3.3 Current Results and Discussions.....	32

3.3.1 Molecular weight of S-PET	32
3.3.2 Morphology -- the TEM results.....	32
3.3.3 Morphology -- the SAXS results.....	33
3.3.4 Thermal analysis.....	39
3.3.5 Hydrogen permeation measurements.....	42
3.3.6 Effects of different clays mixed with PET.....	47
3.4 Conclusions.....	49
 Chapter 4 NEW PEM MATERIALS USED IN FUEL CELLS	 50
4.1 Overview.....	50
4.2 Research Plan.....	51
4.3 Experiments.....	52
4.3.1 Materials.....	52
4.3.2 Method I – PCAS	53
4.3.3 Method II – PCS.....	56
4.3.4 Method III – PASC.....	58
4.3.5 Characterization.....	60
4.4 Current Results and Discussion.....	63
4.4.1 Method I – PCAS.....	63
4.4.2 Method II – PCS.....	73

4.4.3 Method III – PASC.....	79
4.5 Conclusions.....	81
4.5.1 Method I – PCAS.....	81
4.5.2 Method II – PCS.....	81
4.5.3 Method III – PASC.....	81
Chapter 5 CONCLUSIONS.....	82
5.1 Summary.....	82
5.2 Future Work.....	83
List of Reference	85
VITA.....	94

LIST OF TABLES

Table 2-1: Difference among various fuel cell systems	21
Table 3-1: GPC results of sulfonated PET	32
Table 3-2: Onset temperature of S-PET and S-PET nanocomposites	40
Table 3-3: Onset temperature of PET and PET/clay nanocomposites	42
Table 4-1: Molecular weight of linear PCHD	64
Table 4-2: Elemental analysis in Method I	69
Table 4-3: Water-uptake results in Method I	70
Table 4-4: Ionic conductivity results in Method I	73
Table 4-5: Elemental analysis in Method II	76
Table 4-6: Water-uptake results in Method II	77
Table 4-7: Ionic conductivity results in Method II	79
Table 4-8: Elemental analysis in Method III	80

LIST OF FIGURES

Figure 2-1: Four key parts of hydrogen economy	4
Figure 2-2: Three methods of hydrogen production	5
Figure 2-3: Different methods of hydrogen delivery	10
Figure 2-4: Scheme of fuel cell	16
Figure 2-5: Structure of Nafion	19
Figure 3-1: Three types of morphology in PLS	25
Figure 3-2: Photo of mini-extruder (Laboratory Mixing Molder)	29
Figure 3-3: TEM micrograph of S-PET/10% clay nanocomposites	34
Figure 3-4: TEM micrograph of PET/5% clay nanocomposites	34
Figure 3-5: TEM micrograph of PET/10% clay nanocomposites	35
Figure 3-6: SAXS results of PET, PET/5% clay, PET/10% clay, and clay	36
Figure 3-7: SAXS results of S-PET, S-PET/5% clay, S-PET/10% clay, and clay	37
Figure 3-8: SAXS results of S-PET and PET	38
Figure 3-9: SAXS results of S-PET/5% clay and PET/5% clay	38
Figure 3-10: TGA results of S-PET, S-PET/5% clay, and S-PET/10% clay	40

Figure 3-11: TGA results of PET, PET/clay, and clay	41
Figure 3-12: TGA results of S-PET and PET	43
Figure 3-13: TGA results of S-PET/5% clay and PET/5% clay	44
Figure 3-14: Photo of the internal heated high-pressure vessel	45
Figure 3-15: Scheme of Photo of the internal heated high-pressure vessel	45
Figure 3-16: Hydrogen permeability results of PET, and PET/clay	46
Figure 3-17: SAXS result of PET/clay (Closite 10A)	47
Figure 3-18: SAXS result of PET/clay (Closite 15A)	48
Figure 3-19: SAXS result of PET/clay (Closite 20A)	48
Figure 4-1: Photo of crosslinked PCHD membrane	55
Figure 4-2: Photo of PPS membrane with ZnCl_2	61
Figure 4-3: GPC result of PCHD	64
Figure 4-4: ^1H NMR of linear PCHD	65
Figure 4-5: IR of crosslinked PCHD membrane	67
Figure 4-6: IR of crosslinked PPP membrane	67
Figure 4-7: IR of crosslinked PPS membrane	68
Figure 4-8: TGA results in Method I	68
Figure 4-9: SEM of crosslinked PPP membrane (2K)	71

Figure 4-10: SEM of crosslinked PPP membrane (10K)	71
Figure 4-11: SEM of crosslinked PPS membrane (2K)	72
Figure 4-12: SEM of crosslinked PPS membrane (10K)	72
Figure 4-13: IR of crosslinked PCHD membrane	74
Figure 4-14: IR of crosslinked PCHD membrane after sulfonation	74
Figure 4-15: TGA results in Method II	75
Figure 4-16: SEM of crosslinked PCHD membrane after sulfonation (2K)	77
Figure 4-17: SEM of crosslinked PCHD membrane after sulfonation (10K)	78
Figure 4-18: TGA results in Method III	80

ABBREVIATIONS

BHT:	2,6-Di-tert-butyl-4-methylphenol
CHD:	Cyclohexadiene
DABCO:	1,4-diazabicyclo[2,2,2]octane
DCE:	Dichloroethylene
FTIR:	Fourier transform infrared spectroscopy
GPC:	Gel permeation chromatography
HDPE:	High density polyethylene
HFPO:	Hexafluoropropylene oxide
HPLC:	High performance liquid chromatography
IHPV:	Internally heated high-pressure vessel
MCFC:	Molten carbonate fuel cells
NMR:	Nuclear Magnetic Resonance
PAFC:	Phosphoric acid fuel cells
PCHD:	Poly(cyclohexadiene)
PDI:	Polydispersity indices
PEMFC:	Polyelectrolyte membrane
PET:	Poly(ethylene terephthalate)
PLS:	Polymer-layered silicate

PPP:	Poly(phenylene)
PPS:	Sulfonated poly(phenylene)
PS:	Polystyrene
PTFE:	Polytetrafluoroethylene
PVC:	Poly(vinyl chloride)
SAXS:	Small angle X-ray scattering
SEM:	Scanning electron microscopy
SOFC:	Solid oxide fuel cells
S-PET:	Sulfonated poly(ethylene terephthalate)
TEM:	Transmission electron microscopy
TGA:	Thermogravimetric analysis
THF:	Tetrahydrofuran
TMEDA:	N,N,N',N'-Tetramethylenediamine

CHAPTER 1

INTRODUCTION

“Launches a state-of-the-art program to get hydrogen-powered automobiles on the road by 2020 along with the necessary infrastructure to provide for the safe delivery of hydrogen fuels. Establishes an interagency task force on hydrogen as well as an outside advisory committee. Authorized at \$2.15 billion over five fiscal years The program also addresses pipeline hydrogen transmission, convenient refueling, advanced vehicle technologies, hydrogen storage and the development of necessary codes and standards.”

----- Source: Energy Policy Act of 2005

Nowadays, more and more attention is being paid to hydrogen energy research and applications.[1-4] Hydrogen could become one of the dominant energies this century. Researchers in many scientific fields, such as engineering, materials, and the automobile industry are joining the hydrogen system – production, storage, delivery, and end-usage. In the field of polymer science, many novel materials are being developed to feed the needs of the hydrogen economy.

In this thesis, some research work to produce new materials which have the potential use in hydrogen economy will be described. Different analytical methods are used to characterize the new materials.

CHAPTER 2

RESEARCH BACKGROUND

2.1 Hydrogen Economy

In the 19th century, coal was the dominant energy for the steam engine to power the first industry revolution. In the 20th century, oil fueled the internal combustion engine to power automobiles on the road, and then the airplanes in the sky; electricity was used in light bulbs and electrical machines to energize our homes and industry.[5] Now in the 21st century, what will be the next dominant energy source after coal, oil, electricity? The answer could be “hydrogen”!

2.1.1 What is the hydrogen economy?

Hydrogen economy means the hydrogen energy system based on the integrated functional steps: production, delivery, storage, and usage.

Hydrogen exists almost everywhere in our planet, such as in water, natural gas, and oil. It is the most basic element in the universe. There are many different resources to produce hydrogen, and now more than 40 million tons of hydrogen is annually produced all over the world. [6]

Hydrogen can react with oxygen or air to produce clean water and give much heat and energy. Because the product of the reaction is only clean water, not the greenhouse gas

(such as CO₂), byproducts of hydrogen energy would not result in any pollution to our living environment. The use of hydrogen can help us to solve the problem of air pollution and to lower greenhouse emissions.

The heat given out by hydrogen may be efficiently used to empower stationary, combustion engine, and heaters. This makes hydrogen an alternative energy source to petroleum. For example, fuel cell systems using hydrogen as the energy source are now being commercialized in vehicles, and are being introduced to the huge market of home and industrial applications. Up to now, more than two billion dollars have been invested to develop fuel cell vehicles using hydrogen as fuel by famous automakers, such as General Motors, and Toyota. The proton electrolyte membrane fuel cell (PEMFC) gets much attention and is critical to progress in developing vehicles powered by fuel cells. [7] Hydrogen, as a clean and efficient energy, will become an alternative to replace the more and more expensive petroleum in the next decades. It can play an increasingly important role in solving the problems of greenhouse gas emissions and global warming. The hydrogen economy shows huge potential in the energy use because of its environmental and technical advantages. [8]

2.1.2 Four parts of hydrogen economy

There are four key parts in hydrogen energy system: production, storage, delivery, and usage. Figure 2-1 shows the relationship among these four integrated parts.

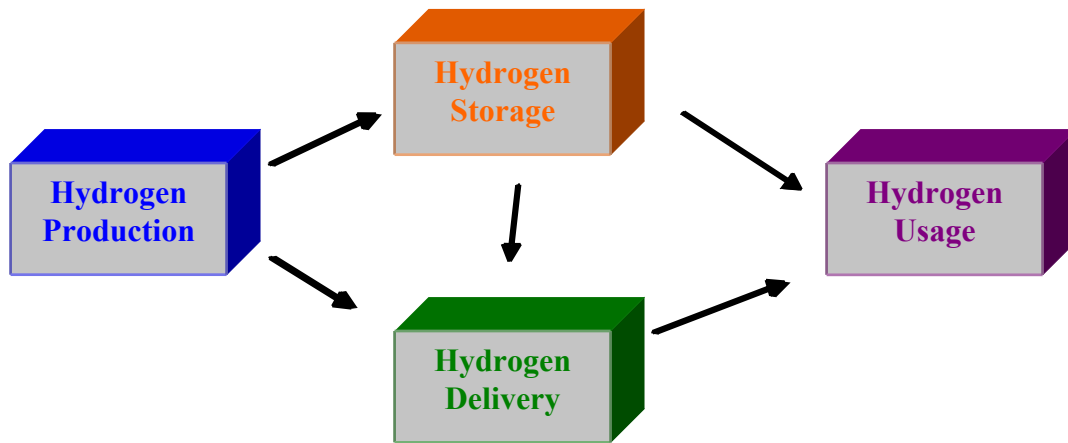


Figure 2-1: Four key parts of hydrogen economy

2.1.2.1 Hydrogen production

Hydrogen exists as a component of air at a very low level of 0.5 ppm. In industry it is produced from some chemical compounds. There are many resources to produce hydrogen by using different technologies based on oil, water, coal, natural gas and so on. Millions of tons of hydrogen are produced in industry each year, and the output of hydrogen will continually increase in the next few years. Three main methods of production are introduced as shown in Figure 2-2: [9]

2.1.2.1.1 Production of hydrogen from fossil fuels

Reaction of fossil fuels with steam can create H_2 , CO and CO_2 . This means we can get the hydrogen from hydrocarbon compounds by steam reforming. Two examples are used

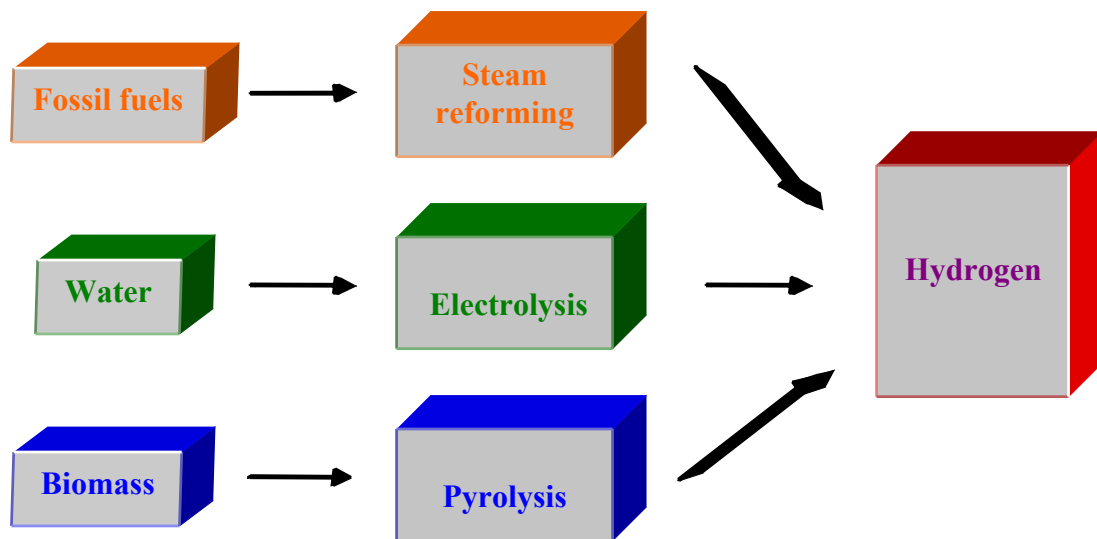
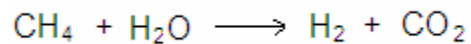


Figure 2-2: Three methods of hydrogen production

to introduce this technology of production -- steam reforming of natural gas, and gasification of coal. [6, 10]

Steam reforming of natural gas

Methane gas -- CH_4 -- reacts with steam over the temperature of $700\text{ }^{\circ}\text{C}$, in the presence of a catalyst, to generate hydrogen. The condition of reaction pressure is between 3 and 25 bars.[11] The reaction formula is shown as:

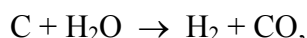


Steam reforming of natural gas is now the cheapest method to produce hydrogen in the mass-production of industry.

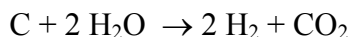
Gasification of coal

Coal when heated up 900 °C converts into the gas phase, and then when mixed with steam generates hydrogen. This reaction can be speeded up if some catalysts like Ni are used. The main products of reaction include H₂, CO and CO₂. [6]

The reaction formula is expressed as:



or



Generally, the products reformed from fossil fuels, such as coal, natural gas or other light hydrocarbons include the mixture of H₂, CO and CO₂. These gases may be separated by the pressure swing adsorption, to get the purified hydrogen. [6]

2.1.2.1.2 Production of hydrogen from water

Hydrogen can be produced from water with solar energy, wind energy, electrical energy or nuclear energy. More than 70% of the area on earth is covered with water; the resource of water is huge and exists almost everywhere. The hydrogen molecule burns with oxygen to give out heat and water. Water can then be split into hydrogen and oxygen by the electrolysis with other renewable energy. This means we can convert all kinds of renewable energy to hydrogen energy via hydrogen molecules. Hydrogen energy never runs out as long as water and any other energy exist. Heat, electricity, light, chemical energy, or even nuclear energy are all used as renewable energy for this purpose. The

reactants and products are both clean water, which has not any impact resulting in environmental pollution.[6, 9]

The reaction formula in this method is shown as below:



The technology of producing hydrogen from water has the greatest advantage in solving current environmental problems because it does not result in any pollution. However, this method has not been very efficient and cost-effective to date.

2.1.2.1.3 Production of hydrogen from biomass

Hydrogen can be produced from biomass by the process of thermal gasification or pyrolysis. Biomass includes straw, sewage, forestry byproducts and so on. [6, 9]

In the process of thermal gasification, biomass is heated up to high temperature, to give out the gas mixtures of H_2 , CO , and CH_4 . CH_4 is then fed with steam to reform into H_2 and CO_2 . After the separation of gas, hydrogen is purified from the gases of CO , CO_2 and CH_4 .

Another process in biomass is pyrolysis which is under development.[6, 9] With pyrolysis, biomass is converted into bio-oil. Then bio-oil is reformed into hydrogen and carbon dioxide. There are many advantages in converting biomass into bio-oil. Bio-oil includes various elements, which can be made into different valuable products. Furthermore, it is easier to transport the bio-oil converted from biomass.

2.1.2.2 Hydrogen storage

Hydrogen can be stored in three different states -- gas state , liquid state, and solid state. [12]

Because the density of hydrogen gas under normal conditions is very low, hydrogen gas is often compressed under high pressure, and then stored in the tanks. This is currently the most mature technology used in the storage of hydrogen.

Hydrogen can also be stored at -253 °C in super insulated tanks by the process of liquidification which makes tanks contain much more hydrogen. Liquid hydrogen requires less volume for storage than gaseous hydrogen does. However, the process of liquidification costs much electrical energy and causes evaporative loss of hydrogen. The energy equal to 30-40% of that in the fuel is needed to cool down hydrogen.[11]

Hydrogen can be stored in the solid state via two different methods -- reversible and irreversible storage. For reversible storage, hydrogen is firstly stored in metal alloy to become hydride, when hydrogen is used, it can be released if the temperature or pressure is changed. The hydride turns back into metal alloy, and then metal alloys have the ability of storing hydrogen again. The storage and release of hydrogen are reversible. For irreversible storage, hydrogen is stored in hydrides, after some reaction hydrides give out hydrogen and react into by-products. However, the by-products can not store the hydrogen to become hydrides again. The hydrogen storage and hydrogen release are irreversible. [13]

There are both advantages and disadvantages in each method of hydrogen storage. Now the compressed gas storage is relatively mature technology, but the volumetric efficiency is still improving. Liquid hydrogen storage is more efficient in volume because its density

is much greater than compressed gas. However, the cost of much energy and restrict requirement ($-253\text{ }^{\circ}\text{C}$) in the process of liquidity hinder the commercial development. Although solid state storage shows some advantages in volume efficiency, more efforts should focus on the challenge of cost, recycling and infrastructure.

2.1.2.3 Hydrogen delivery

Hydrogen delivery includes the infrastructure that transports the hydrogen from the place of production and storage to the end-use devices. Hydrogen is commonly distributed in two states: gaseous hydrogen or liquid hydrogen. [12]

Pipelines are now used to transport gaseous hydrogen, like natural gas, widely. Currently the pipeline is the major and efficient method to deliver hydrogen, and each year about 300 tons of hydrogen is delivered by the pipeline. Because its convenience and efficiency, more pipelines will be used in the large-scale hydrogen delivery, similar to natural gas distribution. Pipelines of hydrogen gas, as the most capable method of hydrogen delivery, will be introduced in more details in the later part of this thesis -- Chapter 2.2.

Gas hydrogen is compressed under high-pressure, and transported by cylinders.

Liquid hydrogen can be delivered in tanks or tube trailers by the road, railway, ship or even air system. But the temperature of liquid hydrogen is below $-253\text{ }^{\circ}\text{C}$, which requires much electrical energy to liquidity and increases the difficulty of handling.

Generally, pipelines are used to deliver gaseous hydrogen to high-demand areas in large-scale, and long distance; while liquid hydrogen is transported to low-demand areas in small-scale by the road system. Figure 2-3 Shows the different methods used in the delivery of hydrogen.

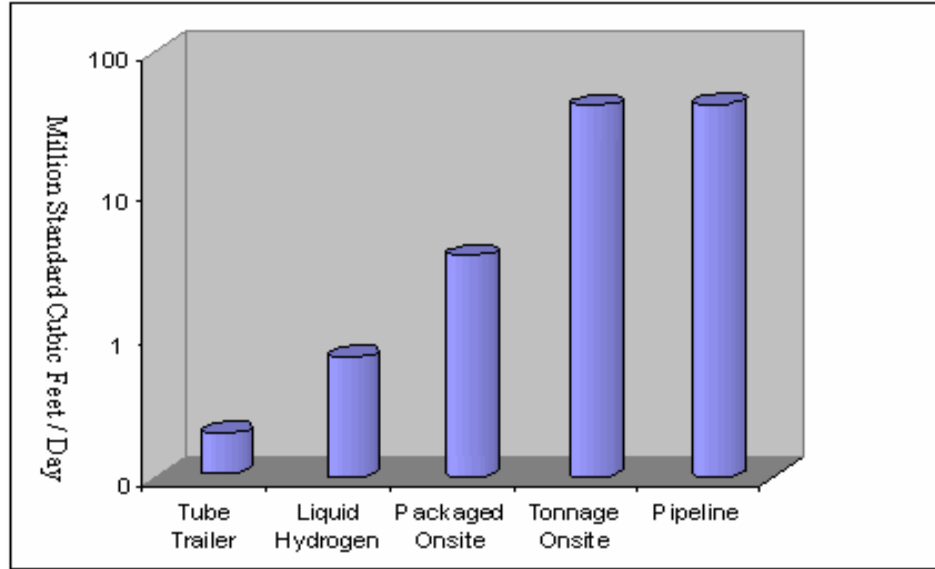


Figure 2-3: Different methods of hydrogen delivery

Source: edited from National Hydrogen Energy Roadmap, Nov 2002, United States Department of Energy [12]

Hydrogen delivery is the key part in commercializing hydrogen energy. In order to solve the technical, environmental and market challenges we are facing, we should develop better components and lower cost for existing transportation system. For example, the lower-cost but higher performance materials for pipeline is needed; hydrogen sensors, and delivery efficiency should be improved.[9]

2.1.2.4 Hydrogen utility

The major objective in the emerging hydrogen economy is that consumers could use hydrogen energy for transportation, portable electronic devices and large power generators to replace the limited amount of gasoline in reserve. The potential market in application of hydrogen is huge. Cost and performance of products used in hydrogen economy should be addressed in the future because consumer market focuses much in the

affordability, convenience, and safety of consumer products. Hydrogen utility plays the key role in the whole hydrogen system, and only if consumers are finally attracted by the hydrogen economy products, the previous investment can be earned back and more funding can be reinvested into the research and application of hydrogen economy.

Transportation

Hydrogen can be used as fuel in internal combustion engines or fuel cells to power the vehicles. Internal combustion engines burn hydrogen, similar to burning gasoline, to give out heat in order to energize the engine. Currently, the technology of using liquid hydrogen in engines is successful in launching space shuttles and rockets. Internal combustion engine automobiles are under the development, and have the potential to become a low-cost alternative to gasoline-fueled vehicles in the near term. They can be made in large-scale to lower the cost of production when the demand continues to increase.

Fuel cells convert the chemical energy to electrical energy to power fuel cell vehicles. For the reason that the electro-chemical reaction is more efficient than combustion reaction in supplying energy, fuel cells can work more efficiently than internal combustion engines do. Many kinds of fuel cell vehicles including buses, trucks, and passenger cars, have been developed and tested by big auto-makers, and some of them are being commercialized.

Fuel cells, playing the most important role in hydrogen energy application, will be introduced in more details in the later part of this thesis -- Chapter 2.3.

Portable electronic devices

Portable fuel cells energized by hydrogen can be used as a battery to power small devices, such as laptop computers, cell phones, and other consumer electronics.

Most of the portable devices use hydrogen or methanol to supply electric power, and methanol can be reformed to provide hydrogen by the reformer. These devices work as battery to provide the electric power of low-voltage and electric flow.

Large power generators

Stationary devices using hydrogen energy are envisioned as the large power generators. They supply the electrical power for buildings, hospitals, and communities. Generally, stationary devices fueled by hydrogen generate power ranging from 2 to 200 KW.

In today's emerging hydrogen energy industry it is eager to develop hydrogen fuel infrastructure technology to generate large-scale power for stationary applications.[6, 9]

2.2 Hydrogen Pipeline

Hydrogen energy could become the next prominent energy source in the near future, but if the hydrogen is applied to the large-scale end-use, then hydrogen infrastructure and delivery network for supplying hydrogen to end-users are requirements in the hydrogen economy.

As far as now, hydrogen pipelines are the best option to transport hydrogen energy, although there is some energy loss, similar to the electric energy loss in the electric power

grids. The method of hydrogen transportation via pipelines is more effective compared with other methods in transporting hydrogen, such as trucks, or tanks. The standard transporting conditions in pipelines are 10-20 bars in pressure, and the regular pipeline material is steel with the diameter of 25-30 cm. [11]

2.2.1 Advantages of hydrogen pipeline

There are many advantages for pipelines to deliver hydrogen over long distance. The lifetime of hydrogen pipelines is long -- over decades, to transport hydrogen energy. The pipelines are paved under the ground, so they are more reliable and safer than any other methods of transportation. And chances of accidents, such as leaking, explosions or environmental disruption could be lower, and pipeline system does not cause further congestion in the road system. Although the one-time fee for constructing pipelines is large, but the maintenance and operational cost are relatively low, and the whole social cost is not very high.

In addition, the mature pipeline system for oil and natural gas has existed for decades. Without change, the mixture of hydrogen and natural gas can be transported via the existing natural gas pipeline system, in which the mole ratio of hydrogen is about 15-20%. With some modifications of lowering carbon content, it is also possible to deliver pure hydrogen in existing hydrogen pipelines. New-built pipelines are made from low-carbon steels, so they can be directly used for delivering pure hydrogen. [13]

2.2.2 Challenges of hydrogen pipeline

When hydrogen passes by pipelines, hydrogen loss happens, similar to energy loss in electric power grids. Therefore, the efficiency in hydrogen pipelines is continually needed to improve.

For natural gas, the pressure in delivery network is low, only about 4 bars. So many cheap polymer materials can be used to replace the expensive steel pipelines. However, because of the low density of hydrogen gas, which is only 1/8 that of natural gas, hydrogen gas should be compressed under high pressure – about 10-20 bars in order to increase the transporting speed. Otherwise, the energy for delivery is not very efficient. Those polymer materials used in natural gas pipelines, such as PVC (Poly(vinyl chloride)) or HDPE (High Density Polyethylene), are too porous to be suitable in transporting high-pressure hydrogen.[7, 9]

Currently, the majority of hydrogen pipelines are made from expensive low-carbon steels. Materials of lower cost than low-carbon steel yet suitable for hydrogen pipelines are a big need in hydrogen economy. Furthermore, if used to transport high-pressure pure hydrogen, these pipeline steels will face embrittlement which results in cracks. These cracks in pipelines would cause serious problems in the delivery of hydrogen.[14-16]

Therefore, in future research directed toward development of the hydrogen economy, low-cost and high-pressure resistant materials are increasingly needed to make the cost of pipelines lower, and allow the commercialization of the hydrogen economy to be realized earlier. In our field of polymer chemistry, there is a lot of potential to develop polymer

pipelines to replace the steel pipelines. Some work in this area was done in this thesis and will be introduced in more details in a later chapter -- Chapter 3.

2.3 Fuel Cells (PEM Fuel Cells)

2.3.1 What is the fuel cell?

Fuel cells are the devices that convert chemical energy of hydrogen into electric energy to produce electric flow. [17]

Fuel cells operate similarly to a battery because both these two devices can convert to the electric energy from chemical energy. But there is obvious difference between fuel cells and batteries. Batteries are more like an energy storage device. After the chemical reactants stored in a battery are used, the battery can not give out the electric energy any more. Only if the battery is charged once more, will the chemical reactants be regenerated and stored in battery. However, fuel cells never run out or need to recharge. Unlike batteries, they produce energy in the form of electricity and heat as long as fuel continues to be supplied. A fuel cell is more like an energy conversion device.

Figure 2-4 shows the mechanism of fuel cell operation. There are two electrodes in a fuel cell -- anode (negative electrode) and cathode (positive electrode); these two electrodes are separated by a membrane. Hydrogen can pass over one electrode -- anode, and react via a catalyst in the anode that converts the hydrogen molecule into a hydrogen ion --

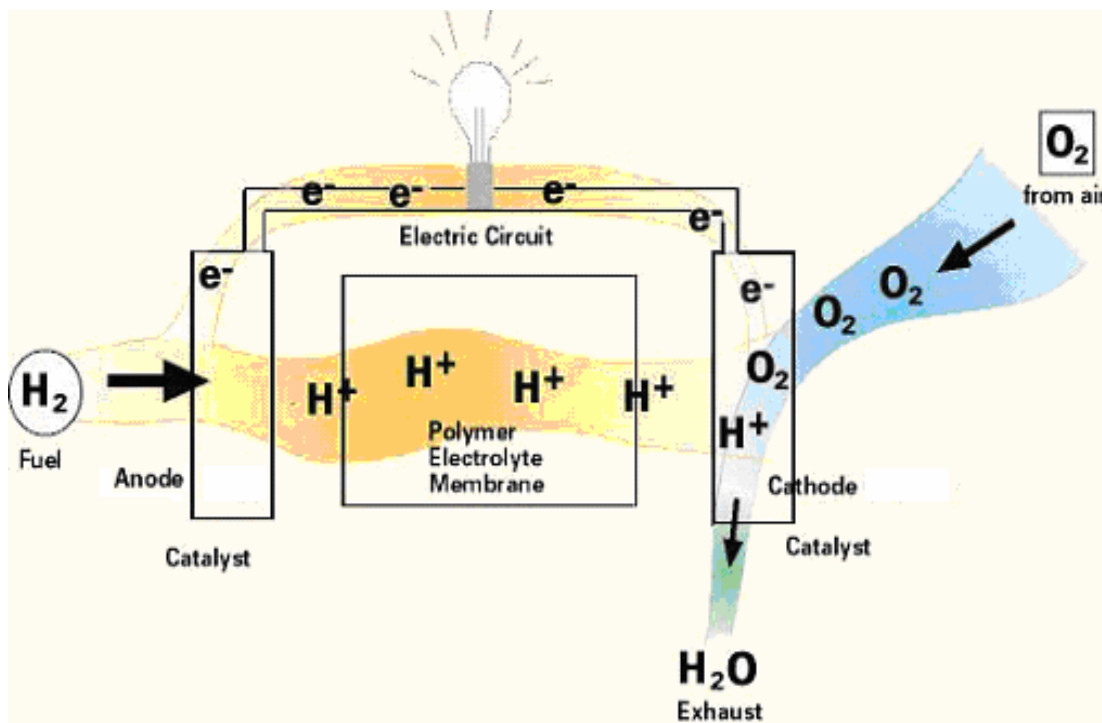
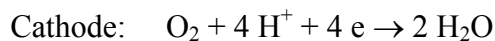
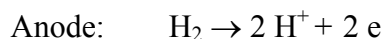


Figure 2-4: Scheme of fuel cell

Source: <http://www.vss.psu.edu/nsf/resources/FuelCell/docs>

proton (H^+) -- and an electron (e^-). The electrons flow out of the cell to become the electrical flow.

Oxygen enters the fuel cell through the cathode. The hydrogen ions then move through the electrolyte membrane to the cathode and they combine with oxygen and electrons to produce water.[17]



Fuel cells are the key application in the hydrogen economy because they can supply the clean, efficient, and fuel-flexible power. Fuel cells can directly convert chemical energy

into electric energy. They have the potential to replace the internal combustion engine in vehicles, and to provide power in both stationary and portable power. [5, 18, 19]

2.3.2 Types of fuel cells

There are several different types of fuel cells, such as polymer electrolyte membrane fuel cells (PEMFC), phosphoric acid fuel cells (PAFC), solid oxide fuel cells (SOFC), and molten carbonate fuel cells (MCFC). Here the PEM fuel cell is emphasized because of its prominent applications. A brief introduction is also given to other types of fuel cells.

2.3.2.1 Polymer electrolyte membrane fuel cells

The application of fuel cell in transportation, such as fuel cell vehicles, is mainly focused on the PEM fuel cell.

Generally, a PEMFC stack contains the following parts: (a). the ion exchange membrane; (b). back layer which is electro-conductive; (c). electrodes between ion exchange membrane and back layer; (d). cell plate which delivers fuel and oxidant to the reactive sites. PEMFC is different from other fuel cells for the reason that the ion exchange membrane is used as the cell separator / electrolyte to separate the reactant gases -- hydrogen and oxygen. The material of the membrane is polymer electrolyte. The structure of the polymer membrane contains ionic groups by which the proton conductivity can take place after the humidification. Therefore, H_2 is oxidized to protons and give out electrons at the anode -- Pt which is deposited on carbon, and protons pass

through the ion exchange membrane, then O_2 is reduced and combined with protons transferred from membrane to produce water at the cathode -- Pt on carbon. The electrons given out flow out to become the electricity.[7, 20, 21]

PEMFC has many advantages over other types of fuel cells, for example it includes high power density capability, fast start, and good response time to load changes. Furthermore, because the separator is polymer membrane, there is no corrosive liquid hazard in the stack, and it is easier to assemble and handle them than other fuel cells. The PEMFC could be made relatively small because of its high power density. All of these characters of PEMFC determine that it can be applied to transportation -- fuel cell vehicles -- well.

Generally, the operating temperature for the ion exchange polymer membrane, such as Nafion[®], in PEMFC is not higher than 120 °C. The low operating temperature is advantageous for the cell can start quickly, but not advantageous for catalyst because carbon could attack the Pt and poison the catalyst. The performance of fuel cell is then reduced. To minimize the effects of CO, the operating temperature should be increased to relatively high temperature.[17]

Currently the most wide-used membrane in PEMFC is Nafion[®] membrane made by DuPont.[22-24] While its operating temperature is relatively low -- less than 120 °C and the cost is still high, it succeeds in making PEMFC practical. Now almost all the commercially available PEMs are based on modified membranes from Nafion[®]. Nafion's structure and properties are briefly introduced in the following.

Nafion[®] PEM

In the late 1960s, DuPont first developed Nafion[®] polyelectrolyte membrane, which is poly(perfluorosulfonic acid) shown in Figure 2-5. The backbone structure of Nafion[®] -- poly(tetrafluoroethylene) is bonded to perfluorinated side chain with a sulfonic acid end group. There are some special properties in Nafion which are important to its use in fuel cells. Nafion is produced by the copolymerization of perfluoro-alkyl sulfonyl fluoride with tetrafluoroethylene. The copolymer is extruded in the melt sulfonyl fluoride to make a membrane, and then this membrane is functionalized by sulfonic acid or base hydrolysis to become the sulfonic acid or salt form.[20]

As a fluoropolymer with good chemical resistance, Nafion is stable thermally and chemically; but with the sulfonic acid end groups in the side chains, ion conductivity can be attained. The ion conductivity depends on the number of sulfonic acid sites, which are hydrophilic. The more sulfonic acid sites, the higher water-uptake degree, and the better the ion conductivity. Therefore, the ion conductivity of Nafion can also be dictated by water-uptake degree.[17, 25]

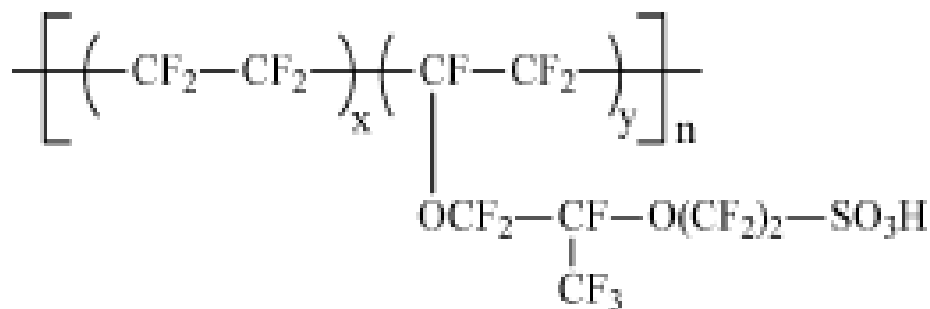


Figure 2-5: Structure of Nafion[®]

Although Nafion membrane exhibits many advantages including high chemical stability and good ion exchange capability, as a proton exchange membrane, it still has some challenges to solve. For example, the present cost of Nafion is high-cost ($> \$800/\text{m}^2$), which limits the further commercialization; and the operating temperature is below 120°C , which reduces the performance of fuel cells.

Therefore, new alternative membranes are needed to increase the operating temperature, and lower the cost of PEM. Some research work about this will be introduced in more details in Chapter 4.

2.3.2.2 Phosphoric acid fuel cells

The electrolyte in PAFC is phosphoric acid, and the operating temperature is $150\text{-}220^\circ\text{C}$. If it is operated at lower temperature, the performance will be reduced because phosphoric acid is a poor proton conductor at low temperature. The expensive Pt is used as catalyst in PAFC. Although the performance of PAFC in selected operating temperatures is relatively high, the cost for this fuel cell system is expensive.

2.3.2.3 Solid oxide fuel cells

Since the 1950s, research on SOFC has been started. The electrolyte is solid metal oxide – $\text{Y}_2\text{O}_3/\text{ZrO}_2$. The temperature of operation is $600\text{-}1000^\circ\text{C}$. Efficiency of SOFC could reach up to 60%, which means SOFC converts 60% of the fuel energy in hydrogen into electric energy in the highest level. [11, 26]

Table 2-1: Difference among various fuel cell systems

	PEMFC	PAFC	SOFC	MCFC
Operating Temperature	80-120 °C	150-220 °C	600-1000 °C	600-700 °C
Electrolyte	Proton exchange membrane	phosphoric acid	solid metal oxide	molten alkali carbonate
Charge Carrier	H ⁺	H ⁺	O ²⁻	CO ₃ ²⁻
Catalyst	Pt	Pt	Perovskites*	Ni

* Perovskites: a large family of crystalline ceramics that derive their name from a specific mineral known as perovskite (CaTiO₃) due to their crystalline structure.

2.3.2.4 Molten carbonate fuel cells

Operating temperature in MCFC ranges from 600 °C to 700 °C. The electrolyte of alkali carbonates becomes molten salt at high temperatures and exhibits ionic conductivity.

Major differences among these kinds of fuel cell systems are listed in Table 2-1.[17]

2.3.3 Applications of fuel cells

Applications of fuel cells are mainly divided into three parts – transportation, portable power, and stationary.[27-30]

For transportation, PEMFC is most commonly used. Passenger cars, buses, trucks and airplanes can all be powered by fuel cell systems, replacing internal combustion engines. It is predicted that fuel cell vehicles will be gradually commercialized in the next few years.

As portable power, fuel cells power laptops or other electric devices like batteries, but they can last longer time in operation than batteries.

In stationary power generation, fuel cells generate electricity to power buildings, schools, and hospitals. The power capacity ranges from hundred of KW to several MW. PEFC, PAFC, SOFC, and MCFC technologies are all used in the stationary power industry.

2.3.4 Future of fuel cells

Because of the obvious advantages in fuel cells -- energy security, high reliability, high efficiency, and high quality of power, fuel cells will have extensive applications in our lives. But there are also problems that need to be solved. More efforts should be focused on cost reduction, increasing power density, extending fuel cell stack life, and improving performance.

CHAPTER 3

NOVEL MATERIALS USED IN HYDROGEN PIPELINES

3.1 Overview

Although there are many different methods of transporting hydrogen on a large-scale, gas pipelines are the lowest-cost means used to deliver hydrogen over long distances. However, the existing hydrogen pipeline technology has not yet achieved the cost and performance goals for successful implementation of hydrogen distribution networks. Some significant technical barriers and economic challenges must be overcome before hydrogen pipeline technology becomes feasible and commercialized. There are two specific requirements for the pipeline technology as follows:

Firstly, we need to develop less-expensive new materials for large-diameter, high-pressure pipelines materials that can resist embrittlement,[14, 15] corrosion, and hydrogen leakage, and perform reliably under harsh operating conditions.

Secondly, there is a need to develop innovative, low-cost leak detection methods such as tracers, and micro sensors.

This thesis describes a research effort that addresses the above needs through the development of new polymers for use as hydrogen gas barriers and the development of advanced polymer composites for constructing non-metallic hydrogen pipelines.

We will work at improving the non-permeability of an established polymer and evaluate its performance as a hydrogen barrier material. Modifications to this polymer promise to

make it perform better than the state-of-the-art barrier materials and thus provide a non-permeable liner suitable for high-pressure hydrogen pipelines.

Due to its excellent gas barrier properties and high strength, poly(ethylene terephthalate) (PET) could be tested and considered as the base material to be modified in the use of hydrogen pipelines. In recent years, polymer-layered silicate (PLS) nanocomposites show improved mechanical strength,[31, 32] thermal stability,[33] gas barrier [34] and high degree of exfoliation[35, 36].

The morphology of PLS nanocomposites plays an important role in achieving such dramatic improvements in properties. Generally, there are three different types of morphology in PLS as shown in Figure 3-1. If the polymer and clay are mixed together as separated phases, it means the clay exists as clusters, and they are not dispersed in the polymer matrix very well.[37] When the polymer and clay are mixed together as the intercalated structure, it results in ordered multilayer structure of alternating polymer chains and clays. When exfoliated structure is formed, it leads to maximize the polymer-clay intercalations and make the entire surface of the clay available for the polymer.[33]

The exfoliated nanocomposites in PLSs can reduce the permeability of gas and fluid through them significantly. The possible reason is called the “tortuous path” mechanism, which means that the clay platelet is non-permeable and thus a diffusing species has a repeatedly altered vector and therefore a much longer path-length.[38]

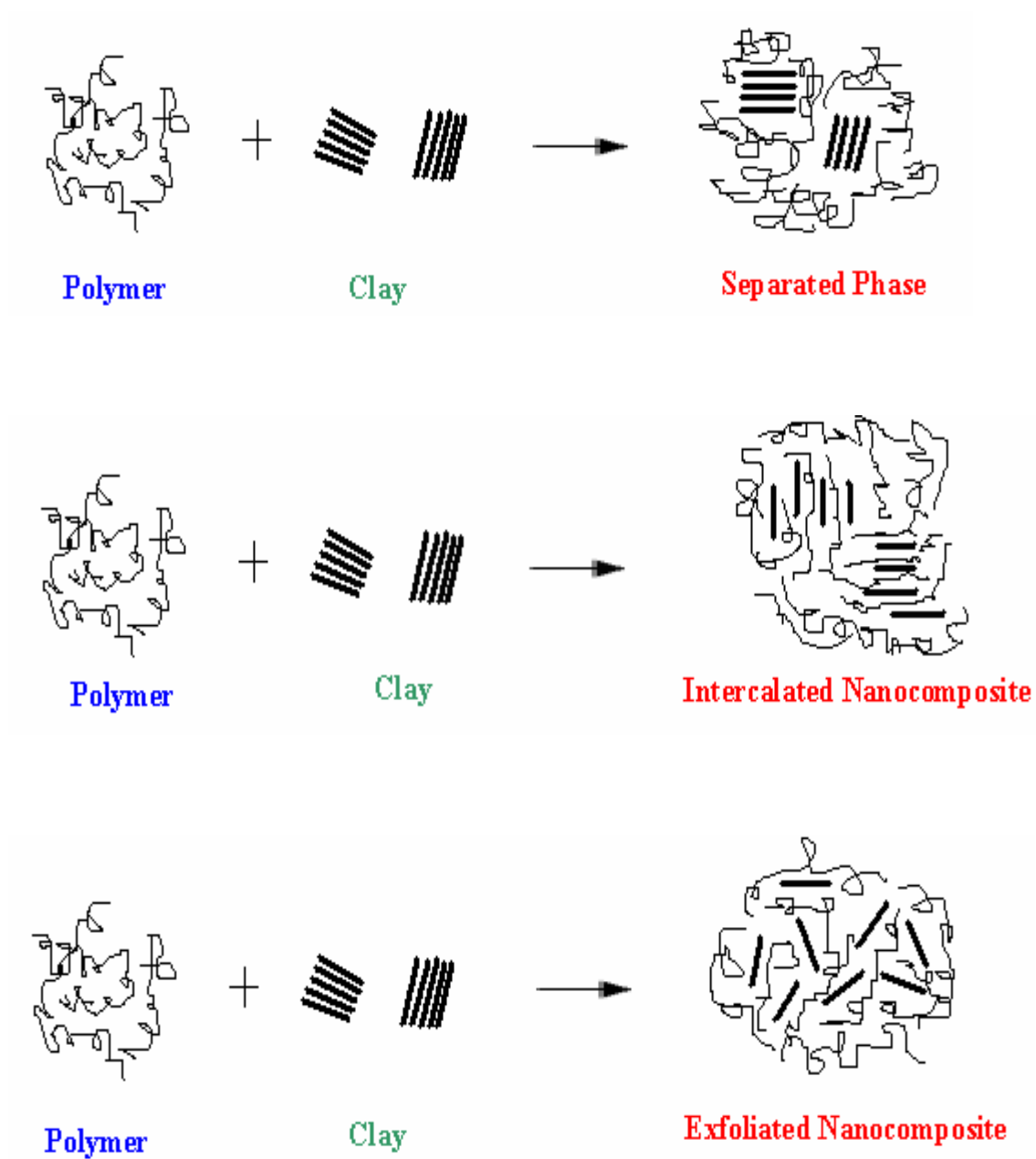


Figure 3-1: Three types of morphology in PLS

In this part of this thesis, our initial effort involves formulating a method for synthesizing PLSs based upon poly(ethylene terephthalate) (PET) and organo-modified montmorillonite and then evaluating their hydrogen permeability and mechanical properties. Some reports on PET/clay [12, 39-43] and PBT/clay[44, 45] have appeared in the literature. In this thesis, solution mixing was used to make PET-PLSs. Sulfonated PET was also mixed with clay for the formation of modified PET/clay. Hydrogen permeability testing was carried out at high pressure over broad temperature ranges.

3.2 Experiments

3.2.1 Materials

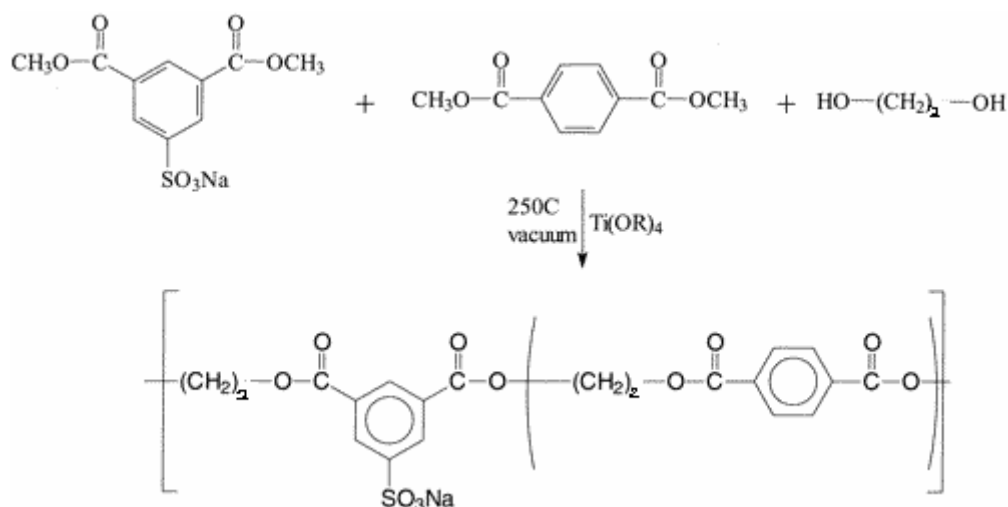
The poly(ethylene terephthalate) (PET) (Eastman 5588 WC) was provided by Eastman Chemical Company. Different alkyl quaternary ammonium bentonites were obtained from Southern Clay Products, Inc. under the names of Cloisite 10A, Cloisite 15A, and Cloisite 20A.

Chloroform in HPLC grade was purchased from Fisher Chemicals, and used as received. Dimethyl 5-sulfoisophthalate sodium salt was purchased from Avocado Research Chemicals, and used as received. Phenol (99+%), dimethyl terephthalate (99+%), , ethylene glycol (99.8%, anhydrous), titanium(IV) isopropoxide (99.999%) were all purchased from Aldrich Chemical, and used as received.

Sulfonated poly(ethylene terephthalate) (S-PET) was synthesized in our lab as the following reports, while some S-PET obtained from the Eastman Chemicals was also used to mix with clays.

3.2.2 The synthesis of sulfonated PET

Sulfonated PET was synthesized by melt condensation polymerization. Dimethyl terephthalate and dimethyl 5-sulfoisophthalate sodium salt with a molar ratio of 97/3, and ethylene glycol were preheated to 130 °C in a round flask with a magnetic stir bar and an addition funnel. Small amounts of catalyst, titanium (IV) isopropoxide were added in and the flask was heated up to 220 °C, then gradually vacuum was applied to remove the extra ethylene glycol. When most of the ethylene glycol was removed, the temperature was increased up to 250 °C under high vacuum for 2 hours. A white solid of PET with a degree of sulfonation of 3% was obtained.



3.2.3 Preparation of PET/clay nanocomposites via solution mixing

Nanocomposites were prepared by solution mixing PET (Eastman 5588 WC) and organomodified clay (Southern Clay, Cloisite 10A) in phenol/chloroform mixed solvent (3/1 weight ratio), while stirring at 70 °C for 3 hours. Two different nanocomposites with clay contents of 5 and 10 wt % were prepared. The solution was dried in a vacuum oven above 85 °C for more than 24 hours.

Other different clays (Southern Clay, Cloisite 10A, Cloisite 15A, Cloisite 20A) were mixed with PET to obtain different nanocomposites via solution mixing same as the above method.

3.2.4 Preparation of sulfonated PET/clay nanocomposites via solution mixing

Nanocomposites were prepared by solution mixing and films were pressed at high temperature and high pressure as we reported above. Two different nanocomposites with clay (Southern Clay, Cloisite 10A) contents of 5 and 10 wt % were prepared and pressed into films.

3.2.5 Preparation of PET/clay nanocomposites via melt mixing

PET and clay (Southern Clay, Cloisite 10A) were also mixed via melt mixing with the mini-extruder (Laboratory Mixing Molder) shown as Figure 3-2. The operating temperature was set at 250 °C, and PET and clay were loaded into the stator cup area after the processing temperature was stabilized. The rotor was then lowered into the cup and mixing began once the samples became melted. Molten PET/clay was mixed at least for 20 mins. Then the rotor was lowered, and the pressure from both the rotor and the extruder pressed the fully molten mixed-PET/clay into the special specimen mold. After the mold was cooled down, the specimens were obtained. The stator cup area of mini-extruder was cleaned with polystyrene for several times.



Figure 3-2: Photo of mini-extruder (Laboratory Mixing Molder)

3.2.6 Material processing

After the dried PET/clay or dried S-PET/clay was produced, they were crushed and ground into tiny particles. Then they were put into the aluminum mold for the process of heat-pressing. Round disks, in which the thickness is 0.03 inches and diameter is 0.41 inches, were obtained by molding samples with the heat-press machine up to 250 °C under high pressure for minutes. The process of heat-pressing should be slow to avoid the air bubbles which could be contained in sample plates. The heat-pressing was repeated until round sample disks plates in good quality were made. The heat-press machine is Carver Laboratory Press (Model C).

3.2.7 Characterization

Gel Permeation Chromatography (GPC)

GPC measurements were performed at ambient temperature in the solvent of methylene chloride / hexafluoroisopropanol (v/v: 95/5) with tetraethylammonium nitrate (0.5 g/l) at a flow rate of 1 ml/min. Molecular weight and polydispersity indices ($PDI = M_w / M_n$) were obtained from GPC relative to calibration with polystyrene (PS).

Transmission electron microscopy (TEM)

Samples for electron microscopy were microtomed in a Leica Ultracut cryoultramicrotome. Sections in approximately 50-100 nm thickness were cut with a

Diatome diamond knife at the sample temperature of -110 °C and the knife temperature of -90°C. TEM imaging was performed on a JEOL 100 CX operated at 100 kV accelerating voltage.

Small angle X-ray scattering (SAXS)

SAXS measurements were carried out by the Molecular Metrology SAXS system. The x-ray source used is a copper microfocused x-ray beam. It is operated at 45 kV and 0.66 mA. The multi-wire detector of the Molecular Metrology SAXS system consists of 2-dimensional array of wires, namely, X- and Y- axis.

Thermogravimetric analysis (TGA)

TGA Q50 of TA Instruments Inc. was used to obtain the thermal behavior. TGA measurements were conducted at the rate of 10 °C/min from room temperature to 600 °C.

Hydrogen permeability

Hydrogen permeation measurements were carried out in an Internally Heated High-pressure Vessel (IHPV). The IHPV can be operated routinely at temperatures between 22 °C and 1000 °C and at hydrogen fugacity as high as 300 MPa.

3.3 Current Results and Discussions

3.3.1 Molecular weight of S-PET

GPC

The molecular weight of sulfonated PET was measured using GPC, and the results are shown in Table 3-1.

The weight-average molecular weight of S-PETs is less than 35 K.

3.3.2 Morphology -- the TEM results

When clay was dispersed in polymer matrixes, two types of nanocomposites could be formed: intercalated structure is obtained when a single extended polymer chain is intercalated between the silicate layers; exfoliated structure is formed when the silicates are uniformly and fully dispersed in the continuous polymer matrix. The analytical

Table 3-1: GPC results of sulfonated PET

Sample Number	Mn	M w	Mz	Mw/Mn
S-PET	8.8 K	30.5 K	51.8 K	3.45
S-PET (A)	11.5 K	34.6 K	55.0 K	3.02

technique of Transmission electron microscopy (TEM) is the best tool for characterizing the structures of nanocomposites.[33]

TEM of S-PET/clay

The S-PET/clay specimens were examined by transmission electron microscopy (TEM). From the TEM images shown as in Figure 3-3, the S-PET appears white and the clay appears dark, and clay was fully dispersed in the polymer of S-PET. S-PET/clay was mainly presented as exfoliating nanocomposites.

TEM of PET/clay

The PET/clay specimens were measured by transmission electron microscopy (TEM). In the TEM images – Figure 3-4 and 3-5 shown below, the PET appears white and the clay appears dark. It is obvious that the majority of the clay is presented as intercalated clusters, with only a partial exfoliation taking place.

3.3.3 Morphology -- the SAXS results

Small angle X-ray scattering (SAXS) analysis was carried out on nanocomposites. SAXS can also give useful information on the morphology of polymer, and show the level of intercalation or exfoliation in polymer materials. For the intercalation of the polymer

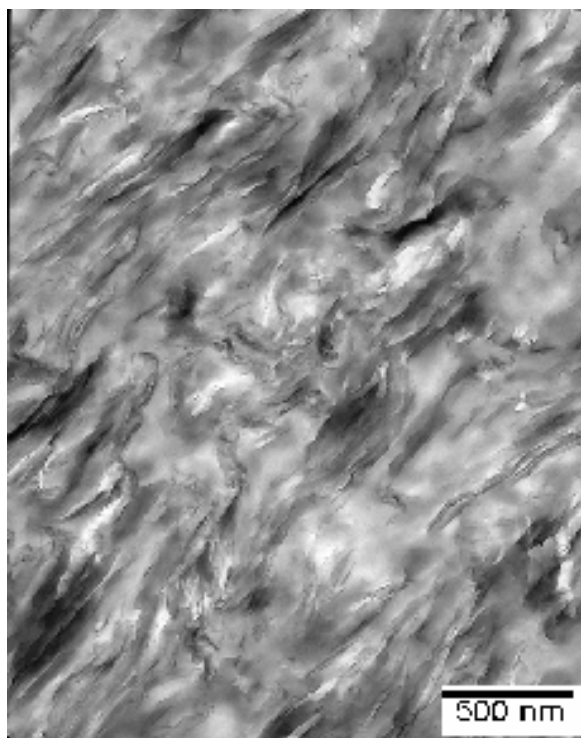


Figure 3-3: TEM micrograph of S-PET/10% clay nanocomposites



Figure 3-4: TEM micrograph of PET/5% clay nanocomposites



Figure 3-5: TEM micrograph of PET/10% clay nanocomposites

chain with clay, it increases the inter-clay spacing and results in a shift of the diffraction peak towards lower Q values ($Q=2\pi\sin\theta/\lambda$) or angle values (θ). In the exfoliated nanocomposite, no more diffraction peaks can be seen in SAXS diffractiongrams of exfoliated structures because the spacing between the clay is too large.[33]

PET, PET/clay, Clay

Four samples of pure PET, PET/5% clay, PET/10% clay, and pure clay, were subjected to small-angle X-ray scattering (SAXS). The results are summarized in Figure 3-6, which plots intensity versus the scattering vector Q . Intercalation of PET chains increases the interlayer spacing of clay, shifting the rather sharp peak to lower Q values as compared to

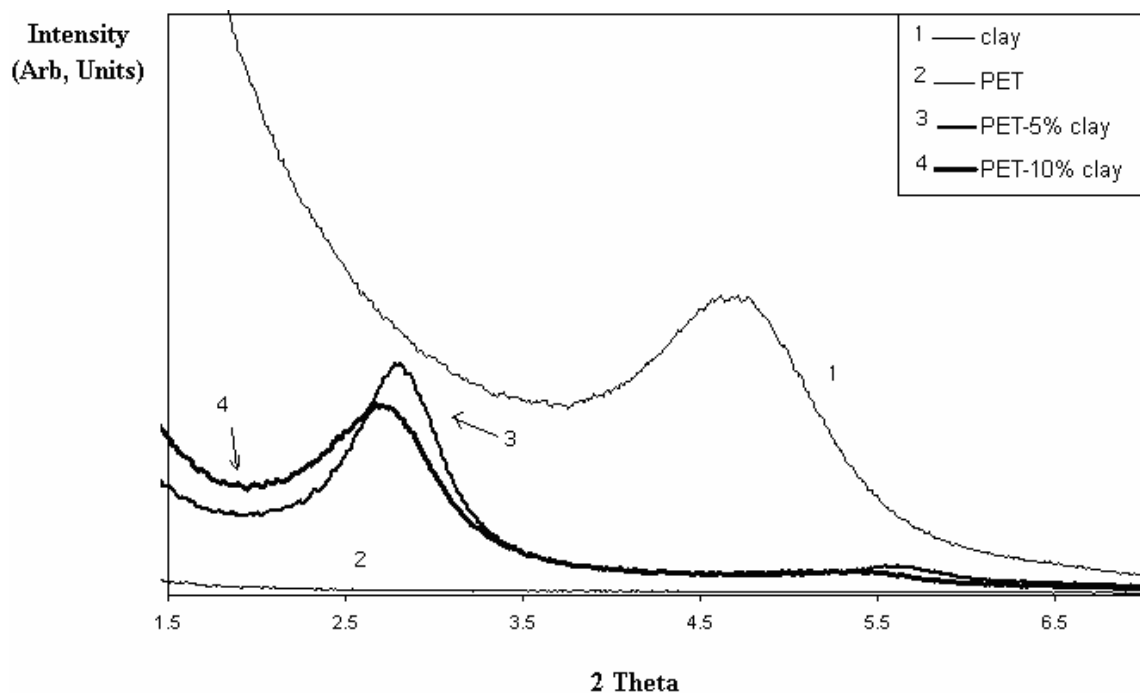


Figure 3-6: SAXS results of PET, PET/5% clay, PET/10% clay, and clay

the pure organomodified clay. The partial exfoliation would result in a more random orientation of the clay platelets and thus a decrease in the sharpness of the peak.

S-PET, S-PET/clay, Clay

Four samples of sulfonated PET (S-PET), S-PET/5% clay, S-PET/10% clay, pure clay were carried out on SAXS. All the results are shown in the Figure 3-7, which compares S-PET from S-PET containing clay. There are broader peaks in S-PET/5% clay and S-PET/10% clay, while the peak in pure clay is very strong between 3.5 and 5.5 at that range. It shows that the S-PET with low level (3% mole ratio) of -SO₃Na and the mixing with clay result in considerable exfoliation.

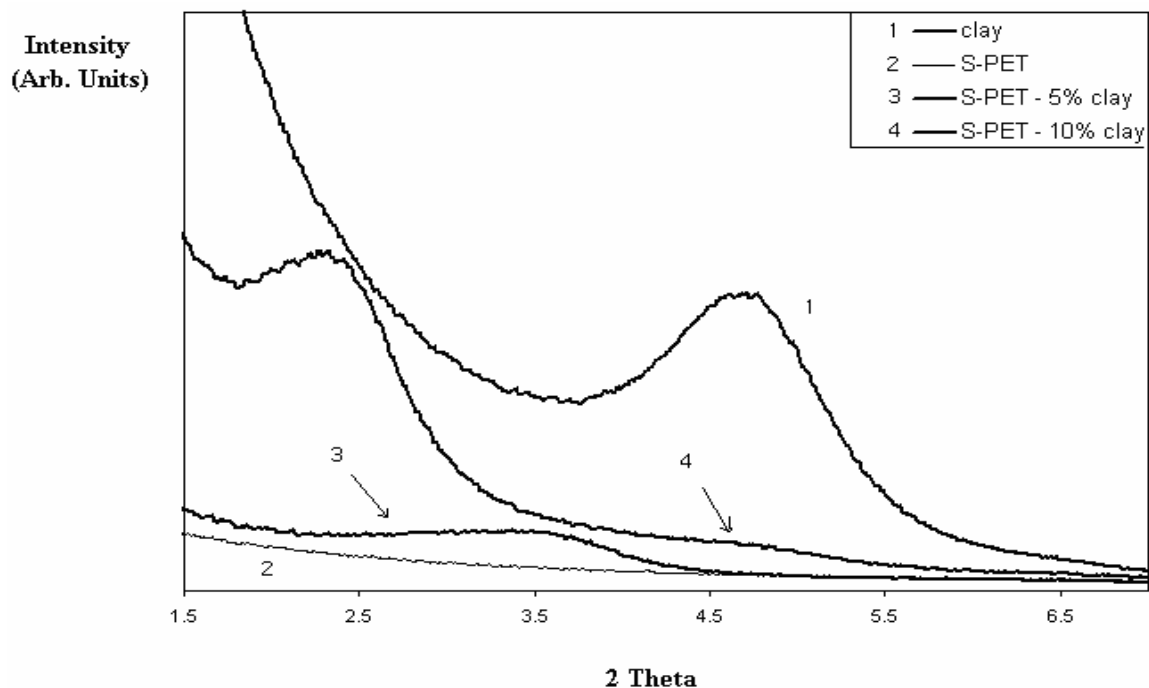


Figure 3-7: SAXS results of S-PET, S-PET/5% clay, S-PET/10% clay, and clay

S-PET and PET, S-PET/clay and PET/clay

Figure 3-8 and 3-9 compare S-PET with PET containing the same amount of clay. The intensity of the main peak drops significantly, which suggests that the number of clay particles giving a d-spacing has decreased much due to the formation of exfoliated nanocomposites. The reason for this probably is that some specific intercalations between the clay surface and PET-SO₃Na increased the exfoliation of nanocomposites.

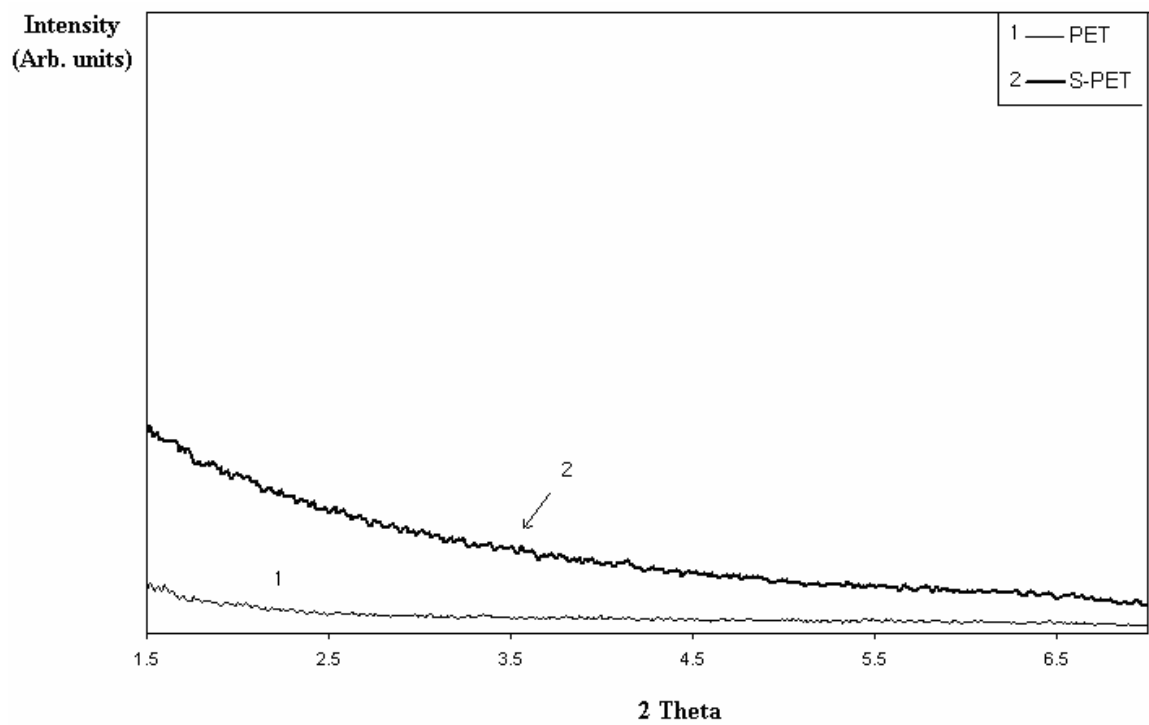


Figure 3-8: SAXS results of S-PET and PET

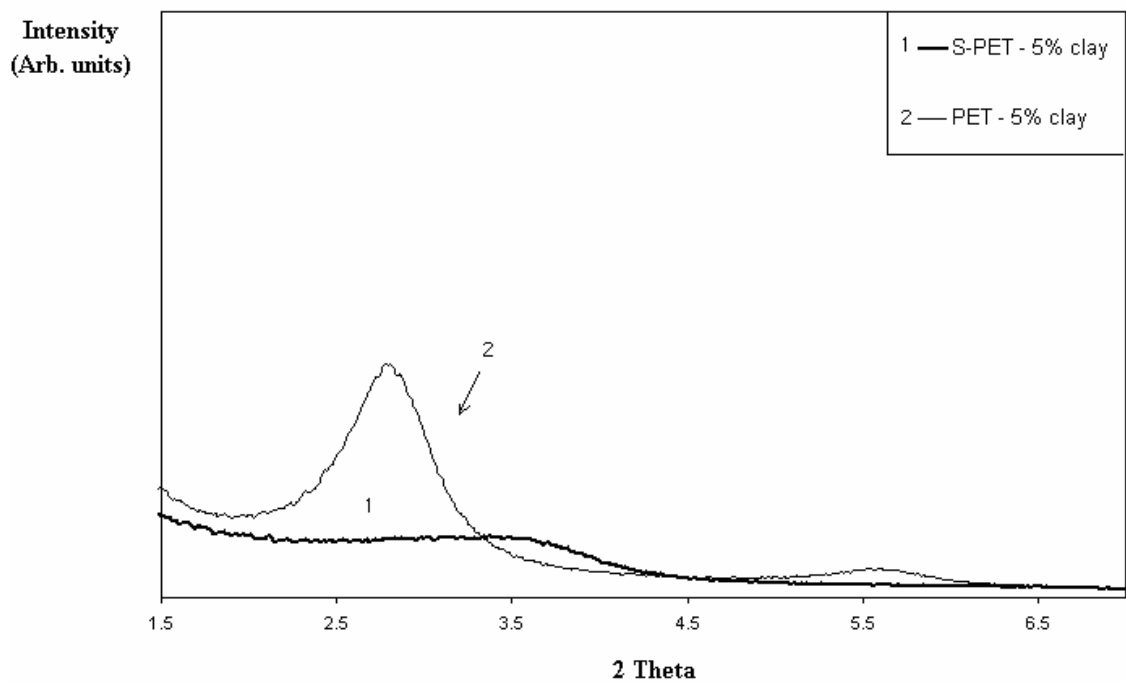


Figure 3-9: SAXS results of S-PET/5% clay, and PET/5% clay

3.3.4 Thermal analysis

We can determine the effect of clay on the thermal stability of S-PET or PET via analysis of thermogravimetric analysis (TGA).

S-PET, S-PET/clay

The S-PET/clay disks were examined by TGA. Compared to their sulfonated PET precursor shown in Figure 3-10, these nanocomposites have slight weight losses from low temperature (100 °C) to their decomposition temperature. Their onset temperatures shown in Table 3-2, 409.51 °C and 405.54 °C for nanocomposites with clay contents of 5% and 10%, respectively, are lower than that of sulfonated PET, which might be related to the weight loss of clay and the mechanical property loss (brittleness) of the nanocomposites. The obtained sulfonated PET and its nanocomposites are a little more brittle than the commercial PET (Eastman 5588WC) and its nanocomposites. It is a big challenge to obtain high molecular weight S-PET by a small batch of condensation polymerization, and low molecular weight could cause low mechanical properties.

PET, PET/clay

The PET/clay disks were tested by TGA. Four samples of PET, PET/5% clay, PET/10% clay, and pure clay are summarized in Figure 3-11. Compared to the blank PET precursor,

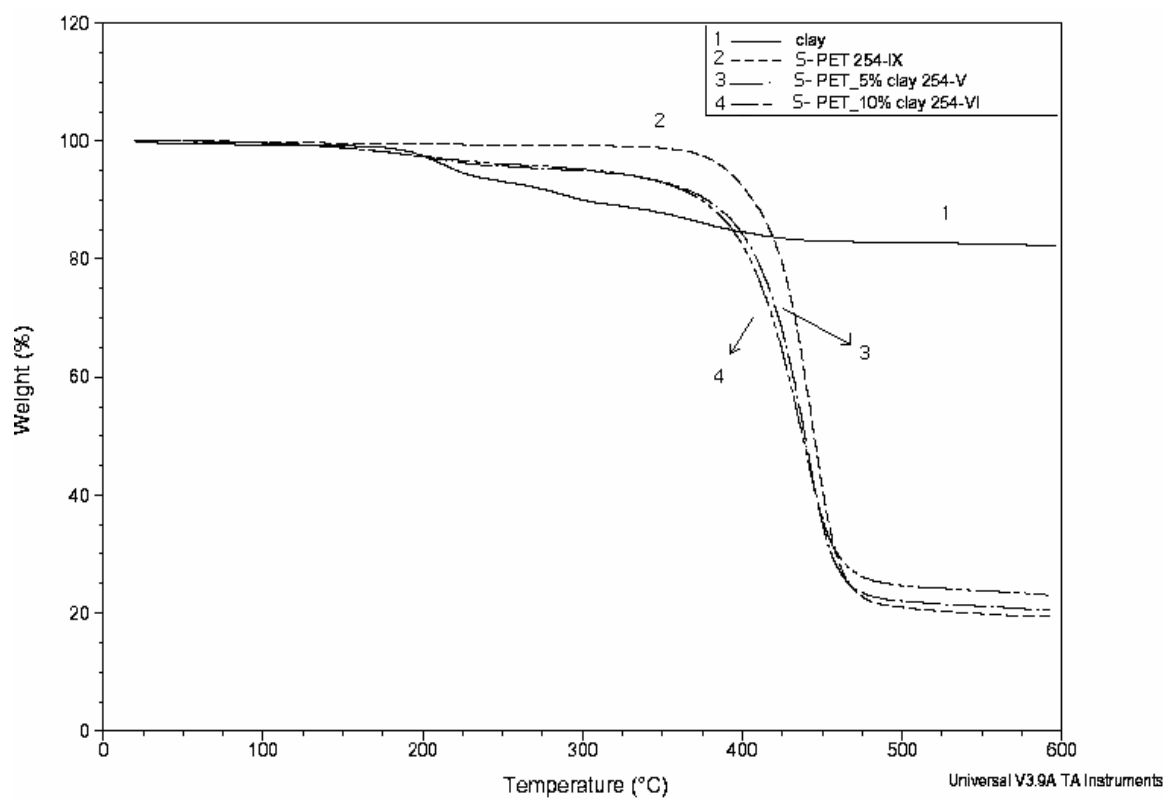


Figure 3-10: TGA results of S-PET, S-PET/5% clay, and S-PET/10% clay

Table 3-2: Onset temperature of S-PET and S-PET nanocomposites

Sample Name	S-PET	S-PET / 5% clay	S-PET / 10% clay
Onset Temperature (°C)	418.89	409.51	405.54

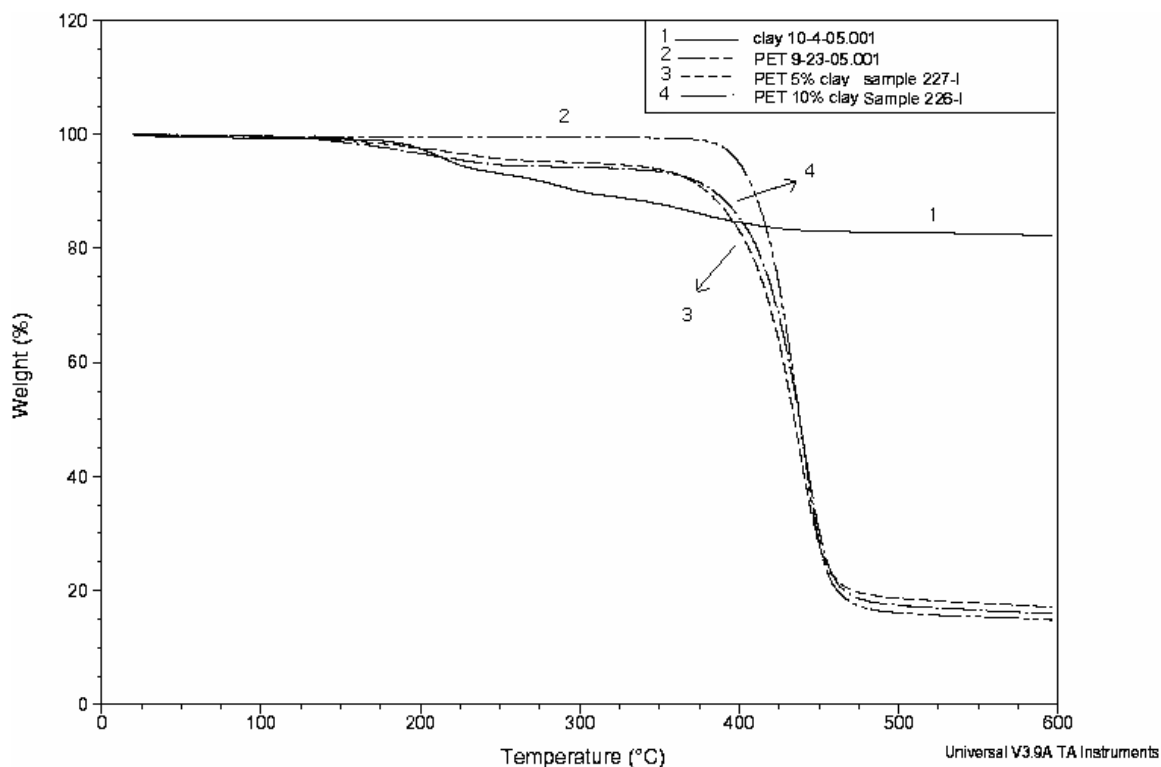


Figure 3-11: TGA results of PET, PET/clay, and clay

PET/clay nanocomposites have slight weight losses from low temperature (100 °C) to their decomposition temperature as shown as in Figure 3-11. For pure clay, there is more weight loss between 100 °C and 480 °C in the results from TGA. The addition of clay to PET caused a slight weight loss in these nanocomposites. The onset temperature of PET and PET/clay nanocomposites are listed in Table 3-3. We found that the higher content of clay in nanocomposites, the higher the onset temperature is.

Table 3-3: Onset temperature of PET and PET/clay nanocomposites

Sample Name	PET	PET / 5% clay	PET / 10% clay
Onset Temperature (°C)	413.28	413.90	415.02

S-PET and PET, S-PET/clay and PET/clay

The TGA results of S-PET were compared to PET in Figure 3-12, and TGA of S-PET/5% clay compared to PET/5% clay in Figure 3-13. Both the results showed that S-PET or S- PET/clay had more weight loss than PET or PET/clay between room temperature and 400 °C. The reason for these results is that the molecular weight of S-PET might be relatively low.

3.3.5 Hydrogen permeation measurements

The instruments for hydrogen permeability are shown in Figure 3-14 and Figure 3-15. Gas permeation experiments were carried out for H₂ at 15.5 °C under an upstream pressure equal to 19.5 bars. The pressure variations in the downstream compartment were measured as a function of time. The permeability coefficient (P) expressed in barrier units

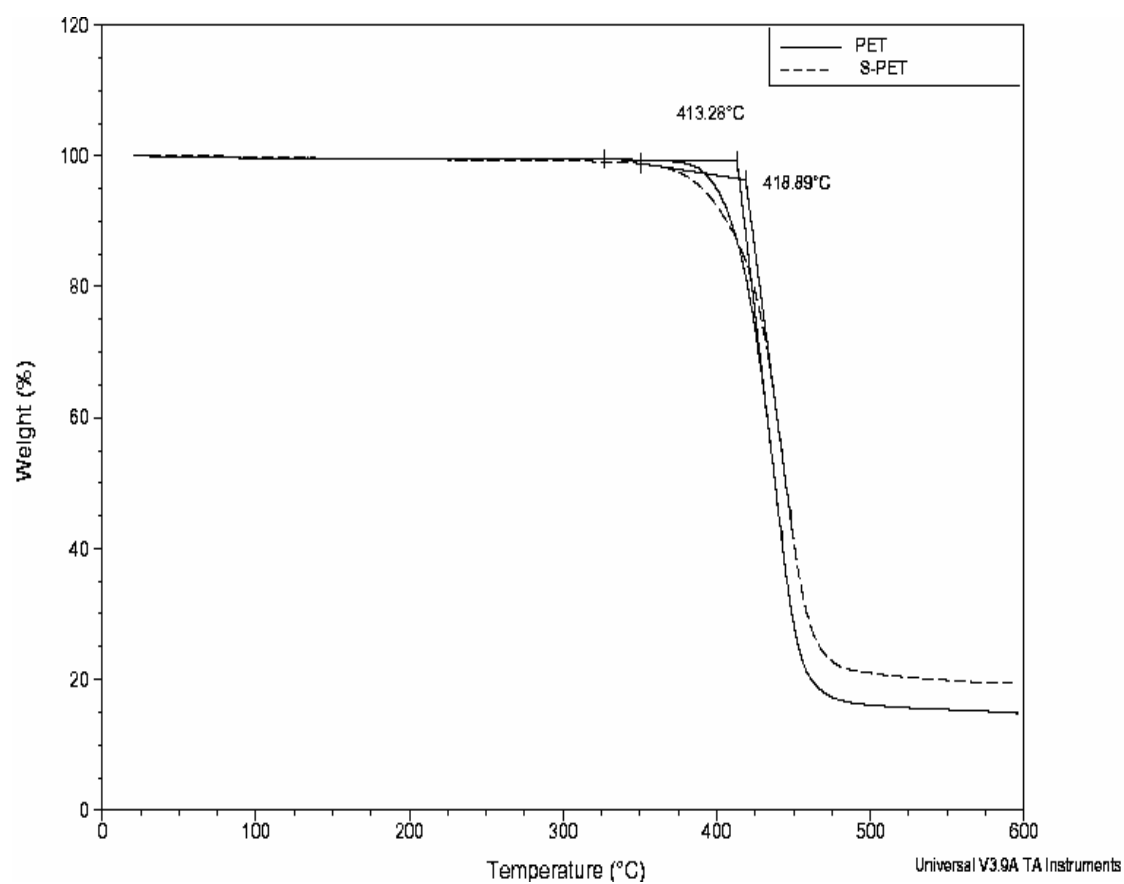


Figure 3-12: TGA results of S-PET and PET

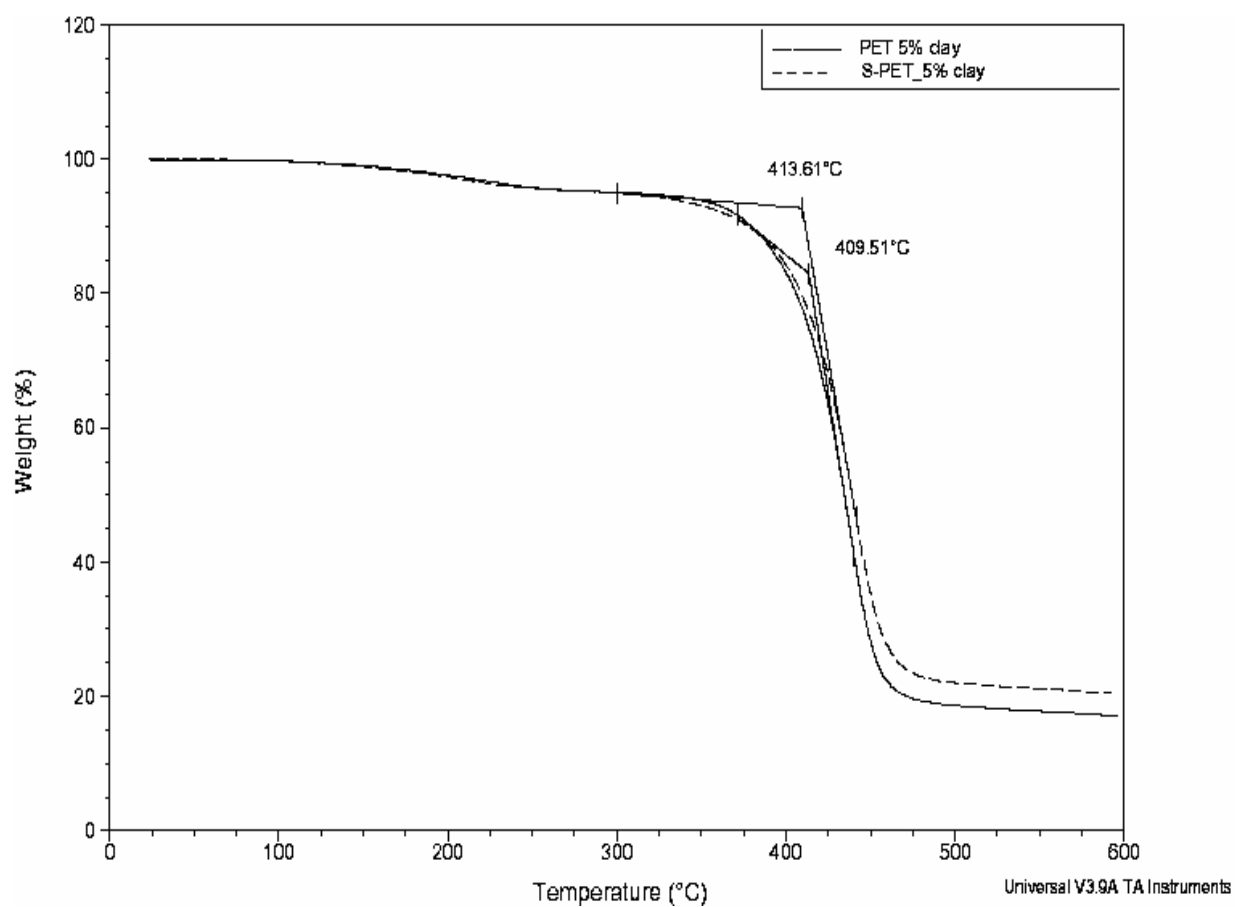


Figure 3-13: TGA results of S-PET/5% clay and PET/5% clay

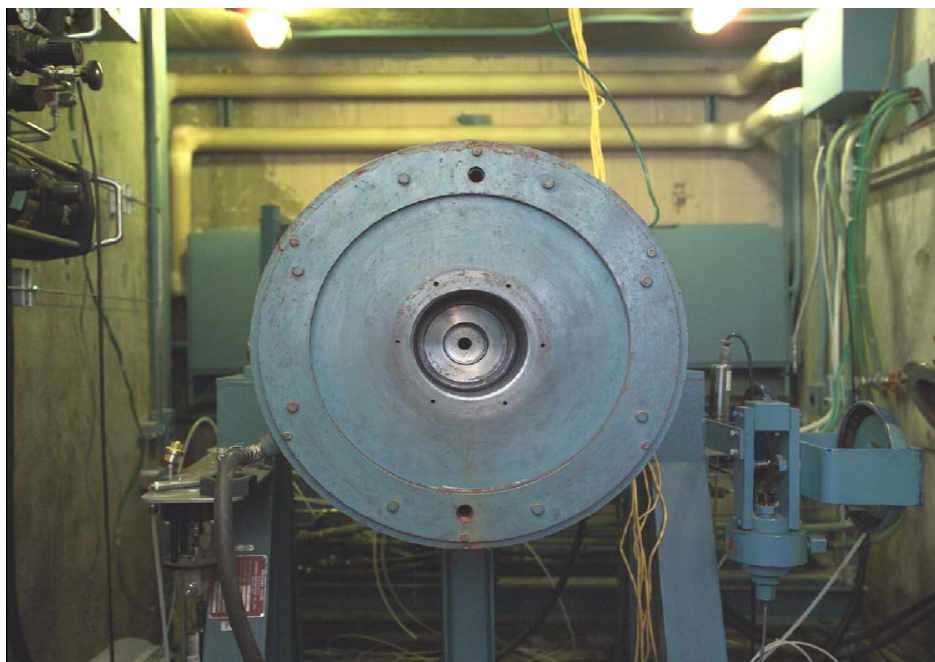


Figure 3-14: Photo of the internal heated high-pressure vessel

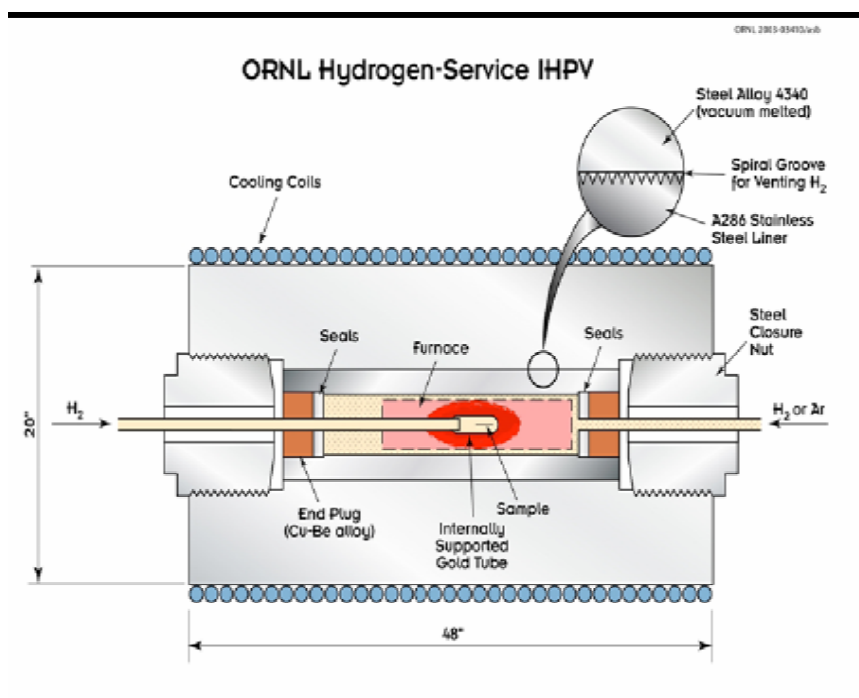


Figure 3-15: Scheme of Photo of the internal heated high-pressure vessel

could be calculated from the slope of the straight line in the steady state. And the diffusion coefficient (D) was deduced from the time lag, θ , which was provided by the extrapolation of this straight line on the time axis.

$$D = e^2 / 6\theta$$

As shown in Figure 3-16, the D of PET is about 5.9×10^{-6} mm²/sec, and D of PET/10% clay is about 2.3×10^{-6} mm²/sec. It is obvious that clay mixed with PET can increase the H₂ gas barrier properties of the polymer.

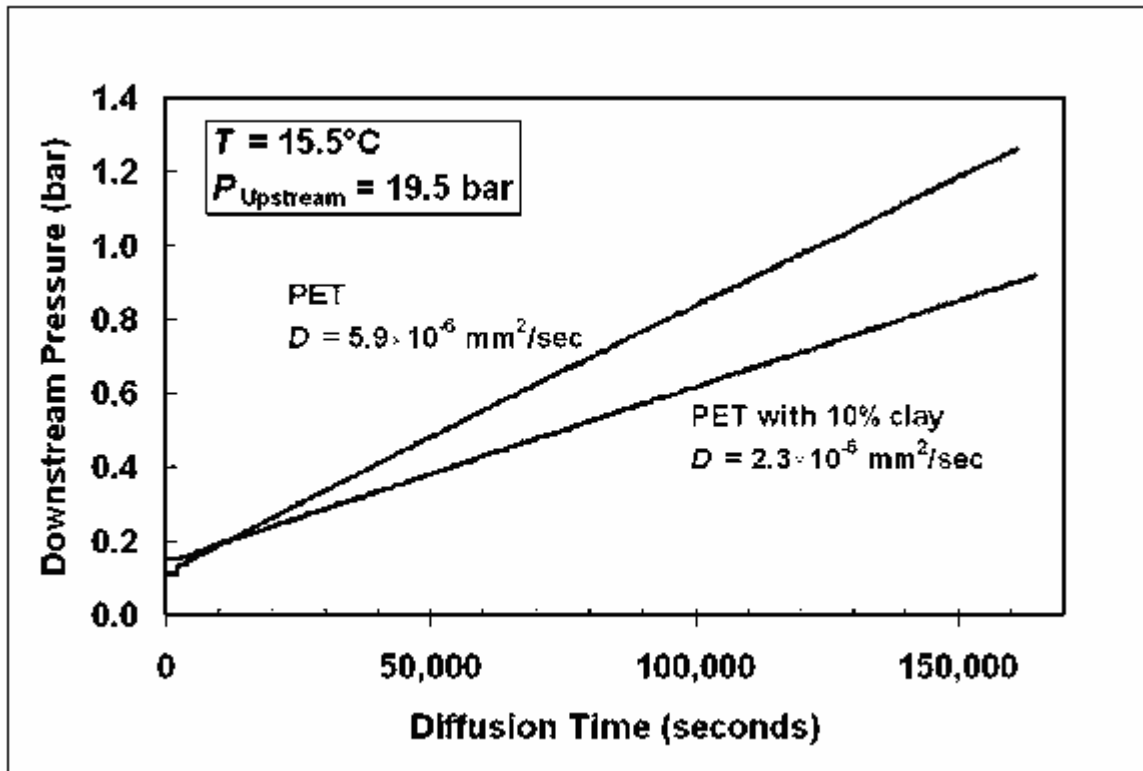


Figure 3-16: Hydrogen permeability results of PET, and PET/clay

3.3.6 Effects of different clays mixed with PET

PET was firstly mixed with different clays (Cloisite 10A, Cloisite 15A, Cloisite 20A). SAXS experiments were carried out to see which ones are most highly exfoliated. The best one could then be mixed with PET or S-PET and measure the H₂ permeability. The SAXS results are shown below.

We can find that the peak between 2 and 4 in X-axis caused by the clay in Figure 3-17 is much smaller and broader than in Figure 3-18 and Figure 3-19. This means the level of exfoliation about clay (Cloisite 10A) mixed with polymer is higher than the other clays.

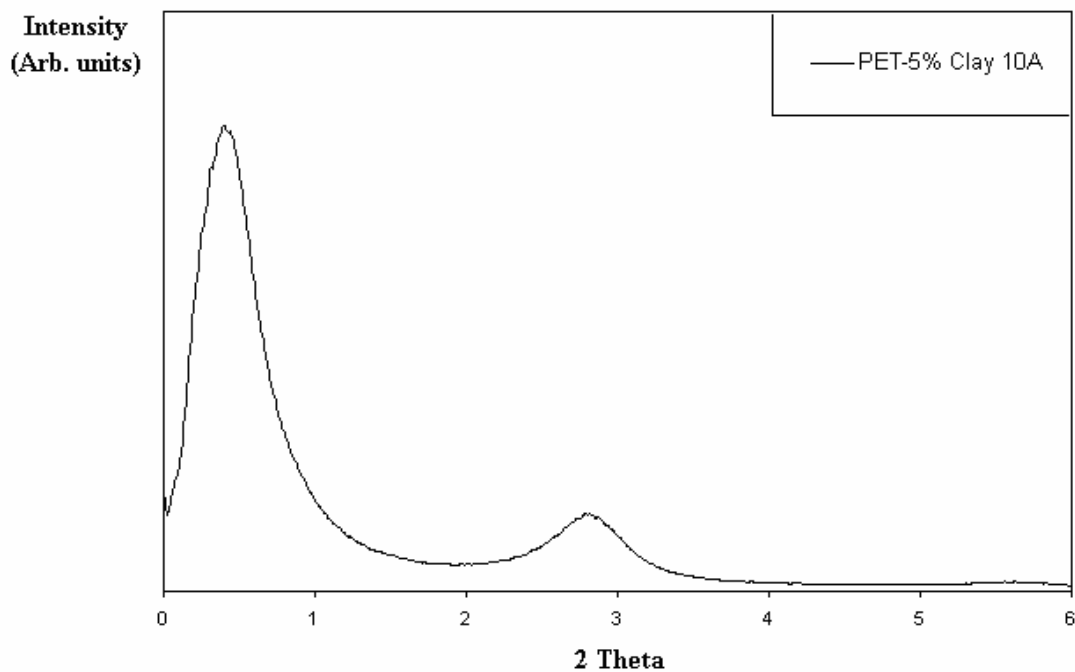


Figure 3-17: SAXS result of PET/clay (Cloisite 10A)

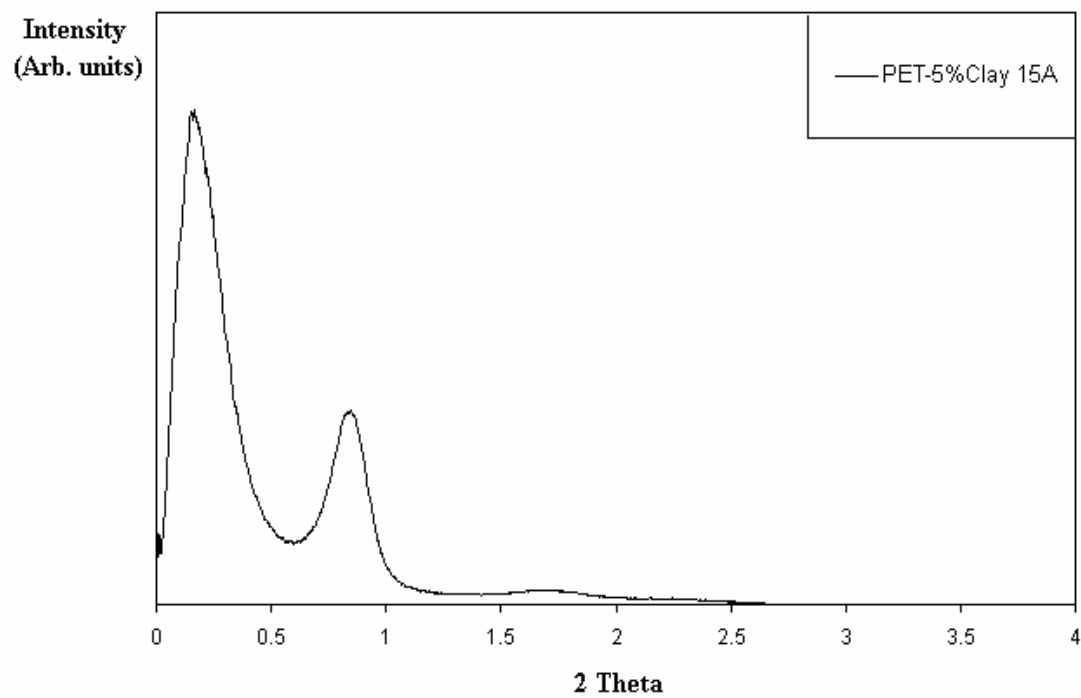


Figure 3-18: SAXS result of PET/clay (Cloisite 15A)

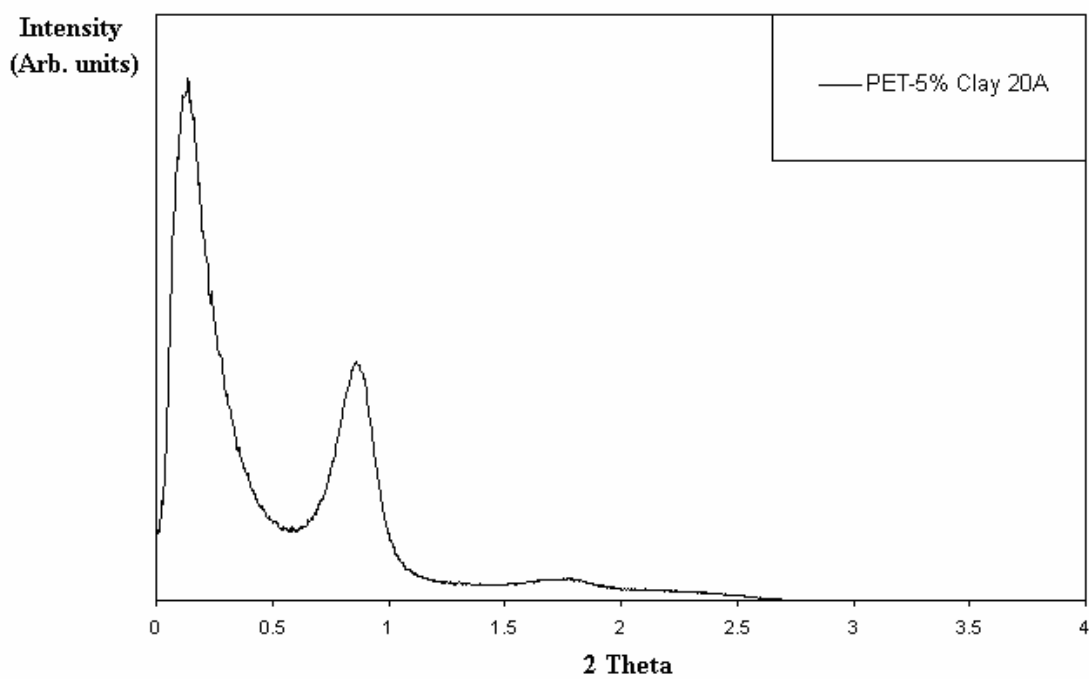


Figure 3-19: SAXS result of PET/clay (Cloisite 20A)

Therefore, we chose the clay (Cloisite 10A) as the one for mixing with polymer material in order to obtain the nanocomposite with highly exfoliation.

3.4 Conclusions

Our effort was to formulate a method for synthesizing PLSs based upon PET and organo-modified montmorillonite and then evaluate their hydrogen permeability and mechanical properties.

PET/clay nanocomposites are promising materials for use in hydrogen delivery due to their low cost, light weight, and ease of processability. A key issue to be addressed is hydrogen permeability. We have demonstrated that addition of clay to PET increases the hydrogen breakthrough time and decreases hydrogen permeability.

Sulfonated PET/clay nanocomposites are highly exfoliated nanocomposites. The SAXS results clearly show the exfoliation in these nanocomposites. Highly exfoliation will enhance the hydrogen barrier property.

CHAPTER 4

NEW PEM MATERIALS USED IN FUEL CELLS

4.1 Overview

Recently much research work has been done on fuel cell systems in hydrogen economy.[5, 7, 17, 19, 22, 46] Proton electrolyte membrane is a key part in fuel cells, and nowadays most of PEM being commercialized are based on Nafion membranes.[20, 23, 47] However, current membranes based on polymers such as Nafion suffer serious disadvantages including high cost ($>\$800/\text{m}^2$) and limited thermal stability at temperatures above 100 °C. PEM fuel cells operating at 80-90 °C are plagued by sensitivities to CO and peroxide formation that limit performance and require the use of high purity fuels.

In this thesis, some work was done to improve PEM materials through novel materials synthesis and characterization. The future goal is the demonstration of capabilities of new classes of PEMs for sustained operation at elevated temperature (150 °C). Polymeric membranes which are able to operate at relatively high-temperature ($> 150\text{ °C}$) would eliminate issues with CO since at this temperature CO absorption is no longer kinetically favorable. The polymeric membrane plays a crucial role in determining the performance of fuel cells.

Poly(cyclohexadiene) offers potential for a unique membrane based entirely on this polymer following several post-polymerization modifications. First, films of the desired

thickness may readily be cast from PCHD solution (ease of processing). The polymer is then covalently cross linked, thus stabilizing the size and shape of the membrane.[48] A chemical dehydrogenation to aromatize the polymer (converting it into poly(phenylene)) using p-chloranil or related reagents is carried out,[49, 50] followed by the sulfonation.[51, 52] The resulting material will be covalently and ionically crosslinked and will have a highly aromatic structure, imparting excellent thermo-oxidative, chemical, and dimensional stability to the membrane. It is believed that these membranes will have the outstanding potential for use in hydrogen fuel cell at temperature well above 100 °C. PCHD, a precursor to poly(phenylene) (PPP), is soluble, tractable, and can be made with controllable and well defined molecular weights by anionic polymerization.[53-55] PCHD has the potential to be an inexpensive commodity polymer with its improved chemical, thermal and mechanical properties.[56, 57] Our strategy is to produce membranes of PCHD by solvent casting, lightly crosslinking the membranes, followed by aromatization and sulfonation. We anticipate the materials to be similar in conductivity to the sulfonated aromatic polymers,[58-60] with enhanced thermal stability, variable chemistry (through copolymerization), and possibly advantages in process ability.

4.2 Research Plan

In this work, some efforts were made to obtain polymer electrolyte membrane based on poly(1,3-cyclohexadiene). These membranes were synthesized by different steps – polymerization, crosslinking, aromatization, and sulfonation. Firstly, linear poly(1,3-

cyclohexadiene) could be obtained from monomer of 1,3-cyclohexadiene; the crosslink reaction which increases the mechanical properties and controls morphology is used to cast membrane; aromatization is made to improve the thermal stability, especially up to 120 °C; sulfonation or adding inorganics is used to increase proton conductivity.

4.3 Experiments

4.3.1 Materials

Some materials were purified to be suitable for the polymerization of PCHD prior to use as the following. Cyclohexane (99%, Fisher) and benzene (99%, Fisher) were purified by stirring with sulfuric acid (10:1 ratio) over 24 hours, then washed with water, 10% sodium hydroxide solution, and water again. The solvents were dried with calcium chloride, refluxed with sodium metal over 24 hours, then distilled under argon just prior to use. 1,3-cyclohexadiene (98%, Aldrich) was stirred with calcium hydride powder over 24 hours at room temperature, then distilled under argon just prior to use. 1,4-diazabicyclo[2,2,2]octane (DABCO), (98%, Aldrich) was purified by distilling (sublimating) from calcium hydride powder under vacuum through a short glass pass, then stored in pre-treated benzene (~ 1.7M). N,N,N',N'-Tetramethylethylenediamine (TMEDA), (99.5+%, Aldrich) was purified by distilling from calcium hydride then diluted in pretreated cyclohexane

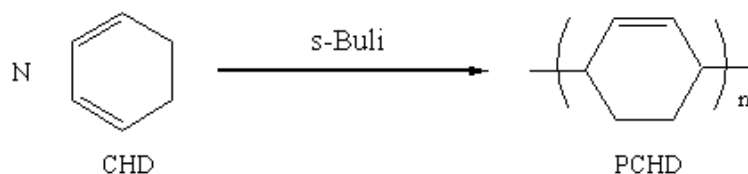
Sec-butyllithium (1.4M in cyclohexane), *n*-butyllithium (1.6M in hexane), and 2,6-di-*tert*-butyl-4-methylphenol (BHT) (99%), hexafluoropropylene oxide (HFPO) (98%), sulfur monochloride (98%), tetrahydrofuran (Certificated), toluene (Certified A.C.S), xylene (98.5%, A.C.S reagent), tetrachloro-1,4-benzoquinone (99%), 1,2-dichloroethane (99%), acetic anhydride (99+%), sulfuric acid (95-98%, A.C.S reagent) were all purchased from Aldrich Chemical Company, and used as received. All glassware and syringes, needles were dried at 150 °C more than 24 hours and cooled under argon protection just prior to use.

There are three different methods we tried to make the desired PEM as described in the following:

4.3.2 Method I – PCAS

PCAS: Polymerization → Crosslink → Aromatization → Sulfonation

Polymerization: to synthesize linear PCHD

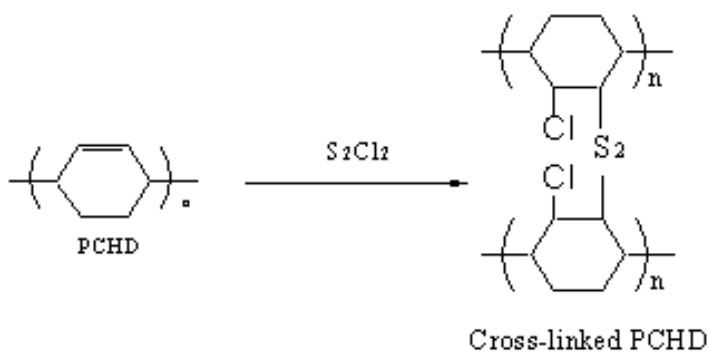


Linear PCHD with highly 1,4 - structure was synthesized under argon atmosphere. A typical synthesis procedure is as following: A 250 mL round bottom flask with a magnetic stir bar was sealed with a rubber septum under an argon atmosphere. 10mL 1,3

cyclohexane (105 mmol) and 1.0mL DABCO in benzene (1.7 mmol) were charged into the flask using syringes and needles together with 150 mL pretreated benzene transferred via double tipped needle. The mixture was titrated with *sec*-BuLi to very pale color then desired amount of *sec*-BuLi (0.4 mL, 0.56 mmol) was injected at one time. The mixture was stirred at room temperature for 4 hours, terminated with several drops of argon purged methanol. The reaction mixture was precipitated in methanol containing 0.02% BHT. After the white precipitate was filtered and washed several times, it was dried in the vacuum oven overnight to obtain the purified linear PCHD.

Crosslink: to cast thin crosslinked PCHD membrane

PCHD of about 2.8 g was dissolved in 35 ml toluene, and about 0.13 ml sulfur monochloride (S_2Cl_2) was dropped into PCHD solution. After stirring of hours, the viscosity of PCHD solution increased, and then the solution were poured into the Teflon



disk. The cross link PCHD membrane was formed in Teflon disk in about 20 hours. The membrane was then evacuated at room temperature to remove the excess solvent on the membrane surface. After the membrane was dried, it was carefully cast as the following picture – Figure 4-1, in which the diameter of Teflon disk was 12 inches.[61, 62]

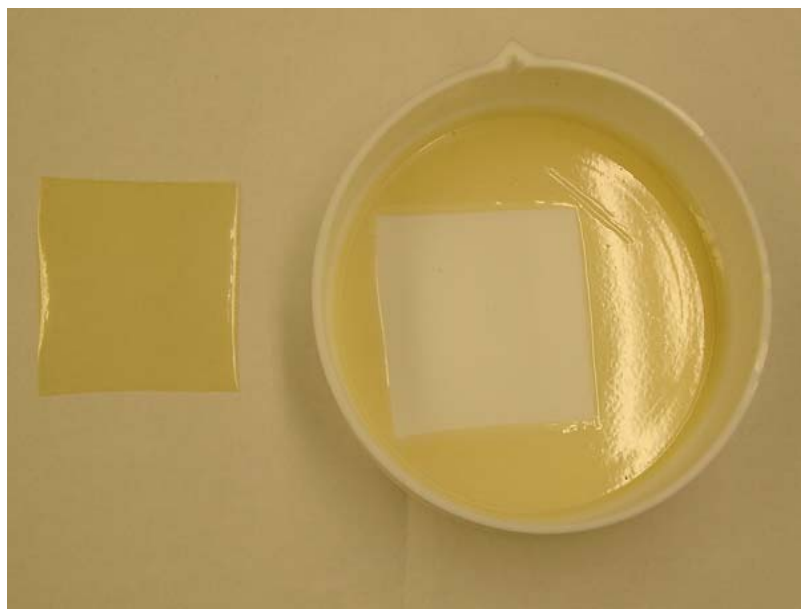


Figure 4-1: Photo of crosslinked PCHD membrane

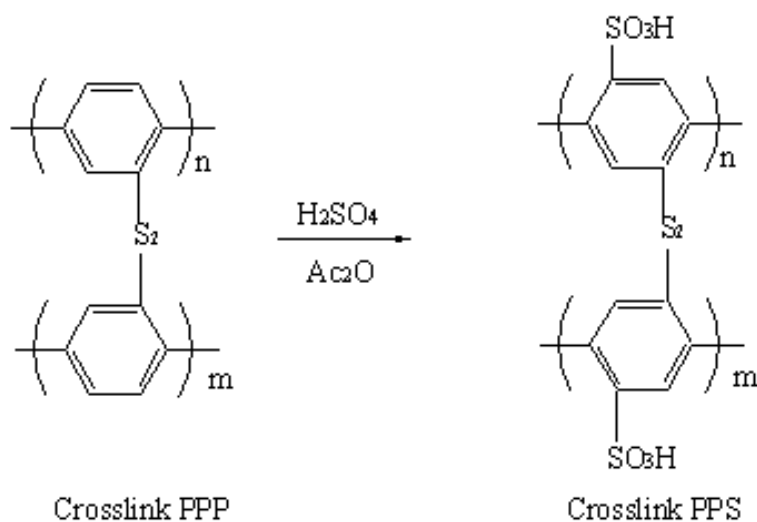
Aromatization: to improve thermal stability & toughness



The above cross link PCHD membrane was put into a three-neck reactor, and reacted with p-chloranil in the solvent of xylene at the temperature of 130 °C. The molar ratio of CHD units and p-chloranil is 1:4. After the reaction of 20 hours, the product of aromatization -- poly(phenylene) -- was cleaned with xylene to remove the excess of p-chloranil.[63] Then the crosslinked PPP membrane was obtained, which appeared dark color.

Sulfonation

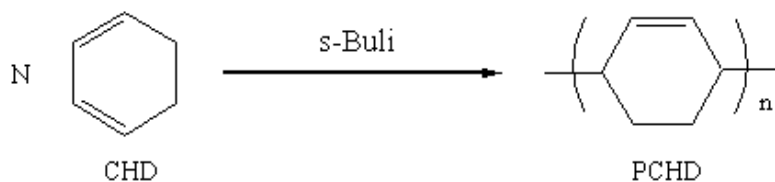
The above crosslinked PPP membrane was put into the solvent of dichloroethylene (DCE), and reacted with the sulfuric acid and acetic anhydride in the atmosphere of N_2 at the temperature of 80-85 °C. The volume ratio of H_2SO_4 and Ac_2O is about 1:1.5. After the reaction of sulfonation, the crosslink PPS membrane we got was washed several times to get rid of the excess reactants. This membrane is the desired PEM which needs further characterization.



4.3.3 Method II -- PCS

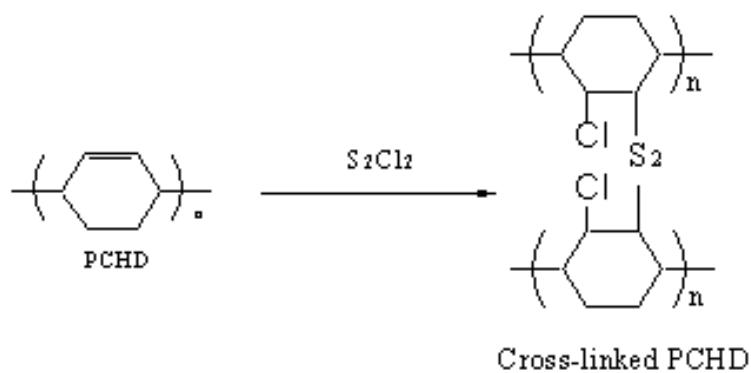
PCS: Polymerization → Crosslink → Sulfonation

Polymerization



The polymerization reacted in the same procedure as in Method I we reported.

Crosslink



The crosslink reaction was same as the procedure in Method I we reported.

Sulfonation

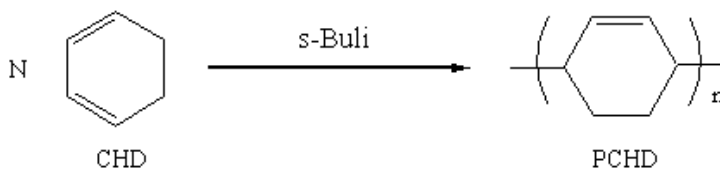
The above crosslinked PCHD membrane was directly put into the solvent of dichloroethylene (DCE), and reacted with acetic anhydride and the sulfuric acid which were dropped by sequence at the atmosphere of N_2 in the temperature of $80\text{ }^{\circ}\text{C}$. The molar ratio of H_2SO_4 and Ac_2O is about 1:1.5. After the reaction of sulfonation over 12 hours, the membrane we got was washed several times to get rid of the excess of reactants. This membrane was another desired PEM which needs further characterization.

4.3.4 Method III – PASC

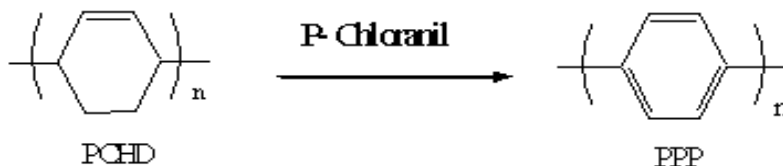
PASC: Polymerization → Aromatization → Sulfonation → Crosslink

Polymerization

The polymerization reacted in the same as the procedure in Method I we reported.

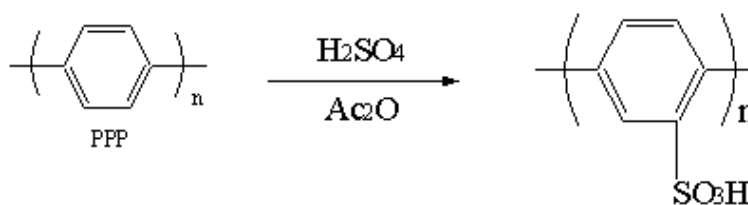


Aromatization



PCHD powder was added into the solvent of xylene in the three-neck reactor, and reacted with p-chloranil at the N₂ atmosphere over the temperature of 130 °C. The molar ratio of CHD units and p-chloranil is 1:4. After the reaction of about 20 hours, the products of aromatization -- poly(phenylene) were filtered to get the raw PCHD. Then it was extracted with the solvent of THF in the extractor at 80-90 °C for about 20 hours to remove the excess p-chloranil. Finally, the products were dried in the vacuum oven overnight to obtain the defined aromatized PCHD (PPP).

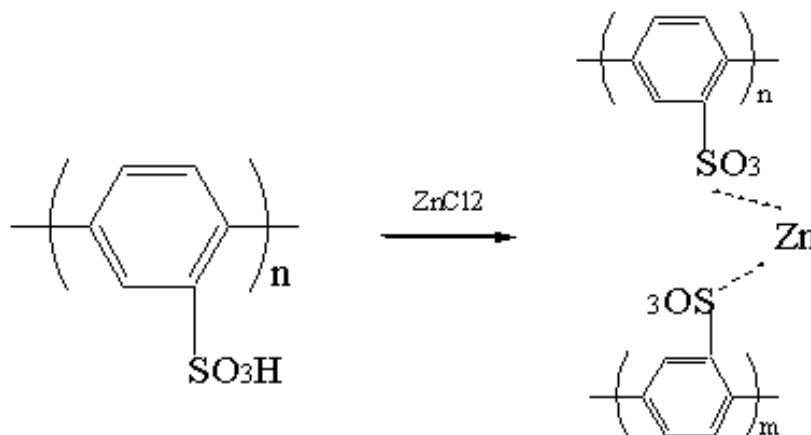
Sulfonation



The above purified PPP powder was put into the solvent of dichloroethylene (DCE) in the three-neck reactor, and reacted with the sulfuric acid and acetic anhydride at the atmosphere of N_2 in the temperature of 80°C . The volume ratio of H_2SO_4 and Ac_2O is about 1:1.5. After the reaction of sulfonation over 12 hours, we purified the crude product of sulfonation using the technique of dialysis tubing. Then they were dried with the frozen dry system for days to obtain the dried powder of sulfonated PPP (PPS).

Adding inorganics

PPS \rightarrow Cross- linked PPS by doped with ZnCl_2 solution as cross-linking reagent[64, 65]



The above PPS powder and zinc chloride in the molar ratio of 1:0.55 were added into the solvent of deionized water. After the stirring over hours, the solution was dried by the frozen dry system. Then the dried mixture shown in the formula was obtained for the next process.

Heat-pressing

The above dried mixture was then pressed into a thin membrane shown as the following picture – Figure 4-2, up to 250 °C with the heat-press machine, under the pressure of 10,000 pounds for about 30 minutes. This membrane is about 0.3 mm in thickness, and 1.5 mm in width.

4.3.5 Characterization

Gel Permeation Chromatography (GPC)

GPC was conducted using a PL-GPC 120 high temperature chromatograph which runs THF at 1 ml/min, 40°C, and a column pressure of 3.1 MPa. The instrument has the following detectors: a Viscotek 220 Differential Viscometer; a Polymer Labs refractometer, and a Precision Detectors PD2040 two angle light scattering detector.

Nuclear Magnetic Resonance (NMR)

¹H NMR measurement was carried out in CDCl₃ at 300 MHz with a Varian spectrometer.



Figure 4-2: Photo of PPS membrane with ZnCl_2

(~1.5 cm wide, <0.3 mm thick)

Elemental Analysis

Elemental analysis was carried out by Galbraith Laboratories, Inc. The elements to measure include carbon and sulfur.

Fourier Transform Infrared Spectroscopy (FT-IR)

Reflectance FT-IR spectra were obtained with a Bio-Rad FTS 6000 spectrometer in the range $4000\text{-}700\text{ cm}^{-1}$, operating at room temperature (256 scans, 4 cm^{-1} resolution).

Thermogravimetric analysis (TGA)

TGA Q50 of TA Instruments Inc. was used to obtain thermal behavior. TGA measurements were conducted at the heating rate of 20 °C/min from room temperature up to more than 600 °C in the N₂.

Water-uptake

Sample were dried in the vacuum oven at 80 °C overnight, after they cooled down, the weight was weighed as W_{dry} . Then the dried samples were added into boiling water for hours, and weighed the weight of the wet sample -- W_{wet} . The weight gain of absorbed water was calculated referring the weight of dried samples: $(W_{\text{wet}}/W_{\text{dry}} - 1) \times 100\%$.

Scanning electron microscope (SEM)

SEM measurements were obtained from LEO 1525 of Oxford Instruments. The magnification is 1K and 20K.

Ionic conductivity

Ionic conductivity of membranes was measured with the equipment consisting of a Battle-designed, 4-point cell and an electrochemical impedance spectroscopy system, which includes a Solartron Analytical SI 1287 electrochemical interface and a Solartron Analytical SI 1260 impedance/gain-phase analyzer. The 4-point cell consists of four 0.5 mm-diameter Pt wires spaced 5mm apart, which are connected to a channeled,

polytetrafluoroethylene (PTFE) housing. The measurement was carried out at both room temperature and 80 °C.

4.4 Current Results and Discussions

4.4.1 Method I – PCAS

GPC of linear PCHD

The weight-average molecular weight of PCHD is about 18.1 K, and PD is about 1.12. The result of GPC is show as Figure 4-3 and Table 4-1. The molecular weight of linear PCHD is not required to be extremely high, or it is hard to control the crosslink reaction of PCHD. The PCHD with too high molecular weight (over 30 K) is very fast to become gel solution and not easy to transfer into Teflon disk to cast membrane in time.

NMR of Linear PCHD

The NMR result of linear PCHD was shown as in Figure 4-4. The assignment of linear PCHD was also shown in the figure below. Most of the linear PCHD we obtained was 1,4-poly(cyclohexadiene).

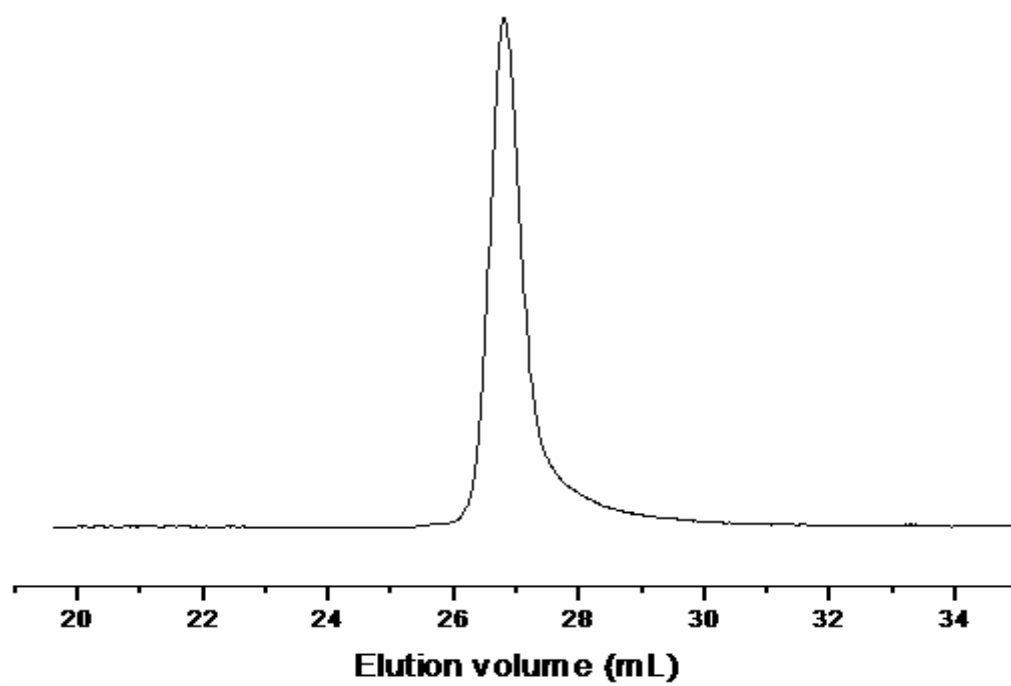


Figure 4-3: GPC result of linear PCHD

Table 4-1 Molecular weight of linear PCHD

Sample Name	Mn	Mw	PD
Linear PCHD	16.2 K	18.1 K	1.12

\

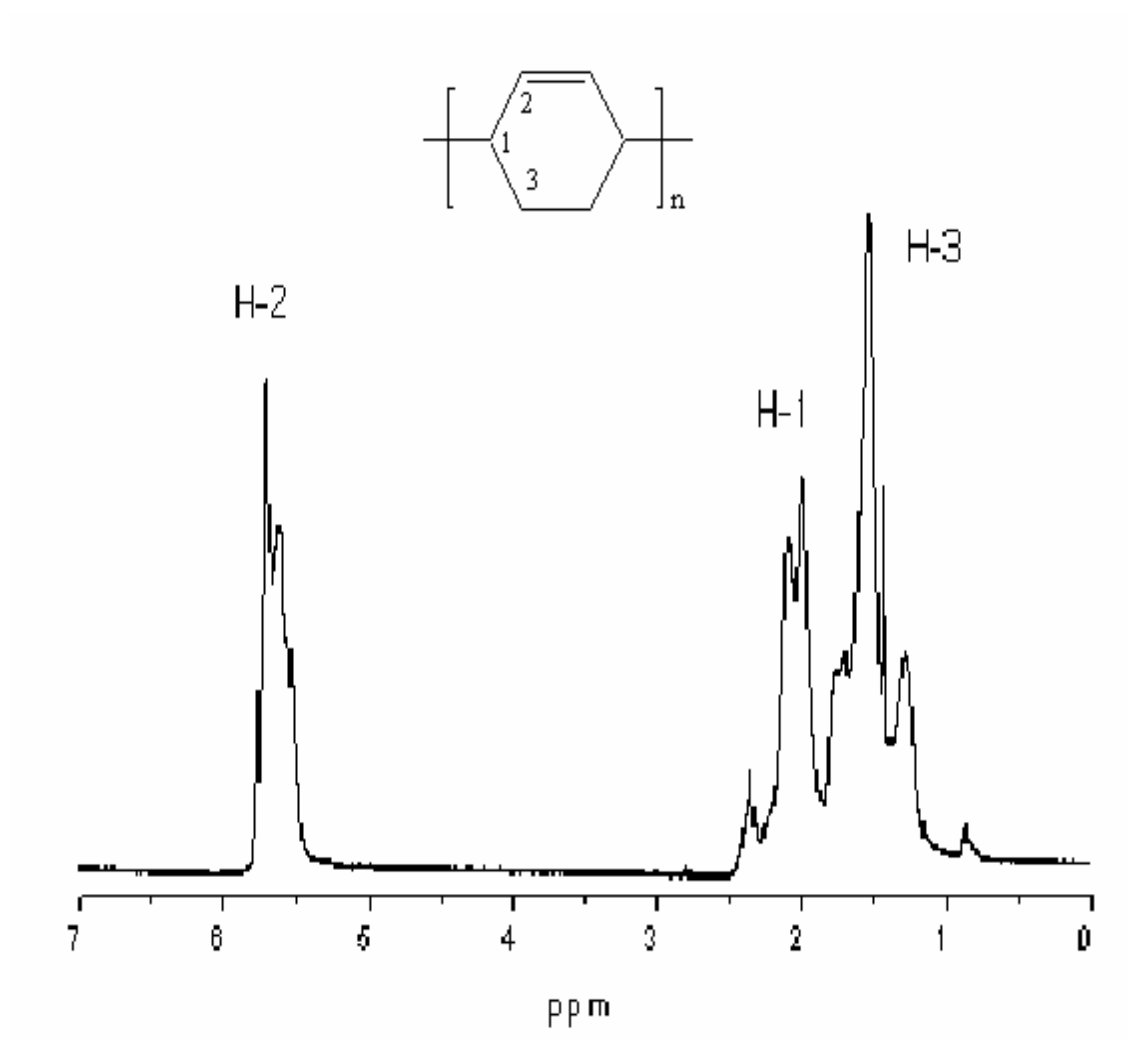


Figure 4-4: ^1H NMR of linear PCHD

FT-IR

A. Crosslinked PCHD membrane (sample 188-I):

After the S_2Cl_2 was dropped into the linear PCHD solution, the transparent solution became a yellow gelled solution and the crosslink reaction occurred. The IR result of crosslinked PCHD membrane was shown in Figure 4-5.

B. Crosslinked PPP membrane (sample 191-I):

The IR of crosslinked PPP membrane followed by the aromatization reaction was shown in the Figure 4-6. Compared with Figure 4-5, the peaks of 3100~3000 (w-m, CH stretch), 1250~1025 (vs, CH in-plane bending) and 770 were assigned to the group of phenyl contained in crosslink PPP.

C. Crosslinked PPS membrane (sample 191-II):

Figure 4-7 showed the IR result of crosslinked PPS membrane. From this figure, we found that the peak of 1250-1150 (vs, S=O stretch) was caused by the sulfonic acid group – SO_3OH ; and 1060-1030 (s, S=O stretch) could be assigned to the group of sulfoxides S=O.

TGA

The TGA results for crosslinked PCHD, crosslinked PPP, and crosslinked PPS are all shown in Figure 4-8. We observe some differences in performance of membranes before

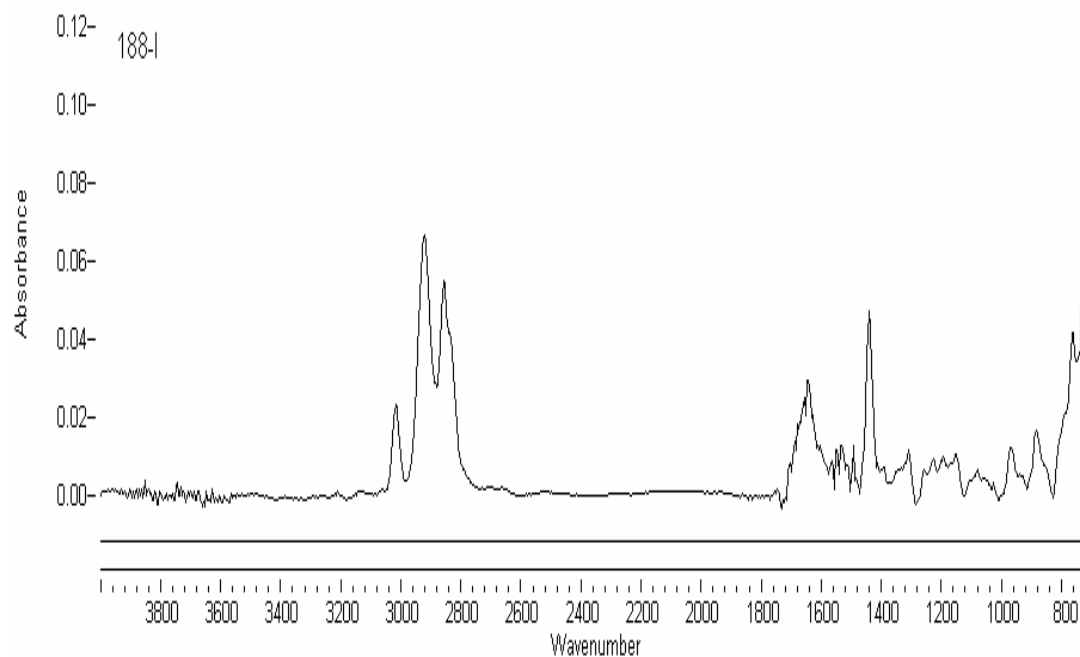


Figure 4-5: IR of crosslinked PCHD membrane

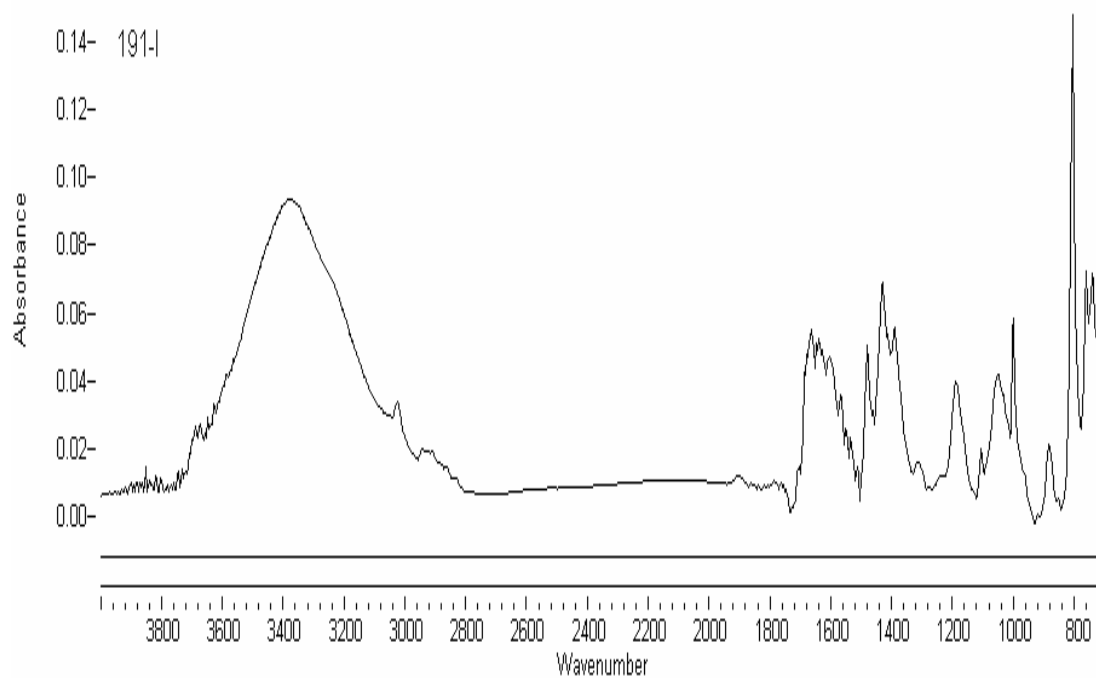


Figure 4-6: IR of crosslinked PPP membrane

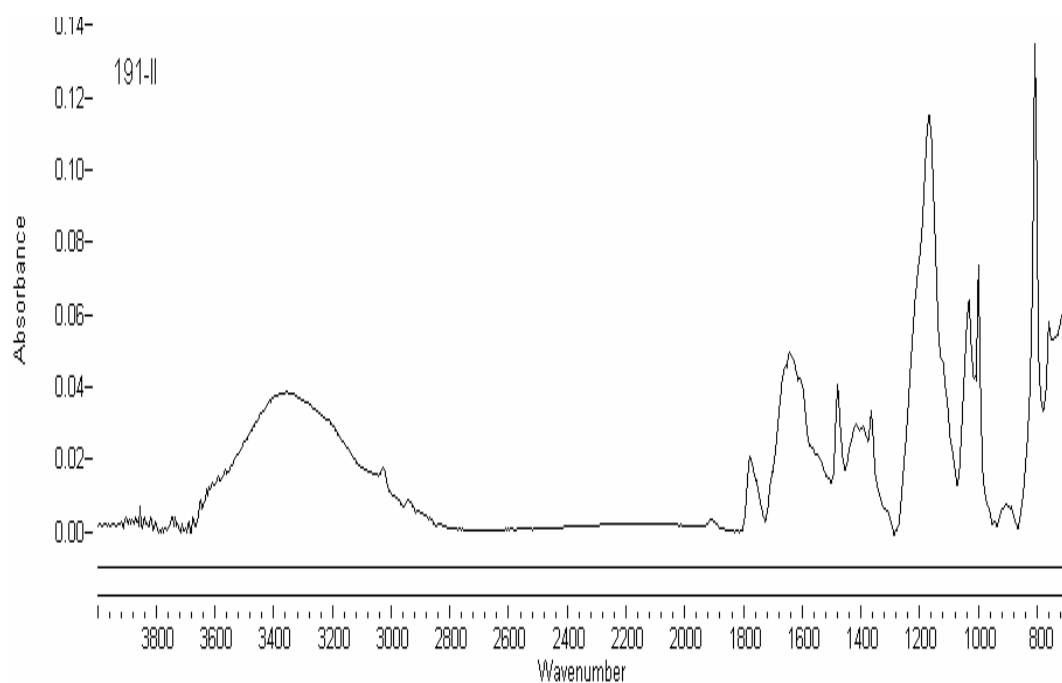


Figure 4-7: IR of crosslinked PPS membrane

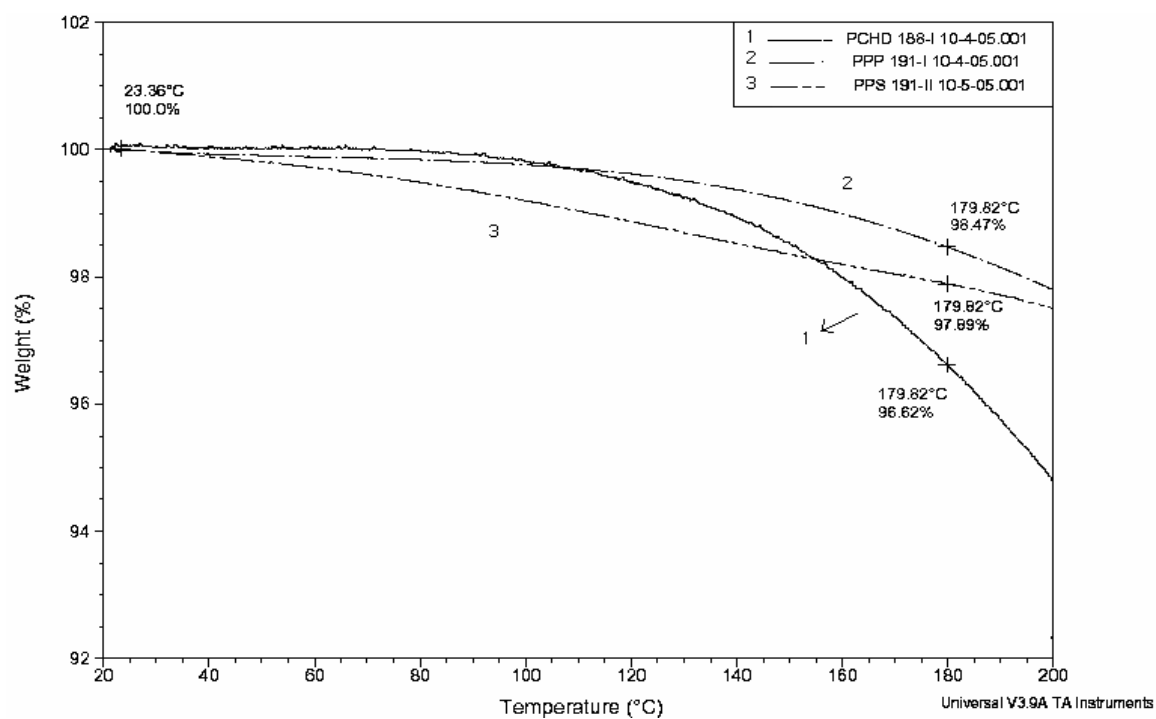


Figure 4-8: TGA results in Method I

aromatization (green line), after aromatization (red line), and after sulfonation (black line). It is obvious that after the aromatization, the thermal stability of membrane became better, and the weight loss between room temperature and 180 °C was less.

Elemental analysis

The elemental analysis of carbon and sulfur in membranes shown as in Table 4-2 were measured. From the molar ratio of carbon/sulfur, we calculated the degree of sulfonation: the sulfonation extent = [(Sulfur/Phenyl in cross-linked PPS) – (Sulfur/Phenyl in cross-linked PPP)] * 100%. In method I, the degree of sulfonation is about 13.1%.

Table 4-2: Elemental analysis in Method I

Sample ID	Analysis	Results
Sample 188-I (after crosslinking)	Carbon%	81.1%
	Sulfur%	5.23%
Sample 191-I (after aromatization)	Carbon%	73.2%
	Sulfur%	3.0%
	Sulfur/Phenyl	0.09
Sample 191-II (after sulfonation)	Carbon%	60.1%
	Sulfur%	6.0%
	Sulfur/Phenyl	0.22

Table 4-3: Water-uptake results in Method I

Sample ID	Weight (before in boiling water)	Weight (after in boiling water)	Weight increase %
Sample 191-II (after sulfonation)	0.019 g	0.021 g	5.3%

Water-uptake

The content of water-uptake increases with the increase of degree of sulfonation. Therefore, from the results of water-uptake as shown as in the Table 4-3, we can confirm the reaction of sulfonation.

SEM

Crosslink PPP membrane (Sample 191-I):

Figure 4-9 and 4-10 show the surface morphology of crosslink PPP. Figure 4-9 is the SEM picture in the magnification of 1:2000, and Figure 4-10 is in 1:10000. The white points are caused by the dirty spots in the membranes.

Crosslink PPS membrane (Sample 191-II)

Figure 4-11 and 4-12 show the surface morphology after sulfonation. Figure 4-12 in higher magnification could show the difference of membrane surface after the sulfonation.

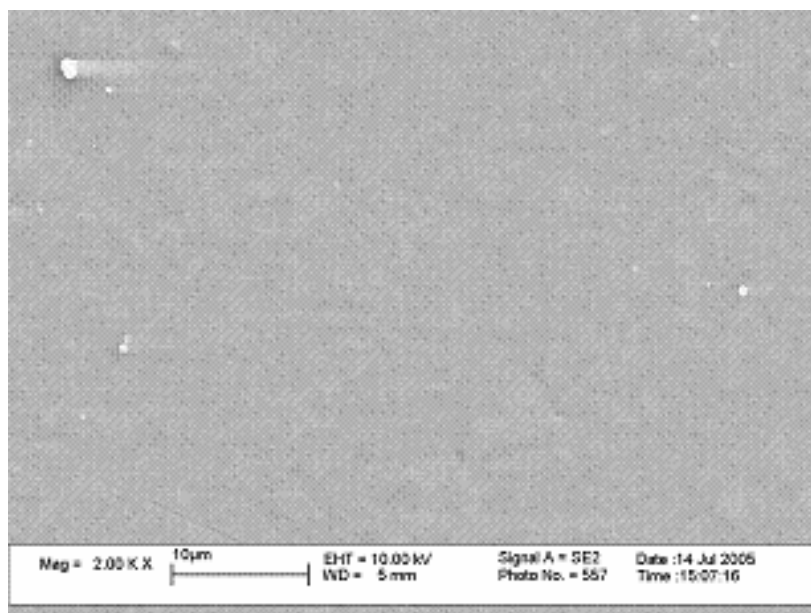


Figure 4-9: SEM of crosslinked PPP membrane (2K)

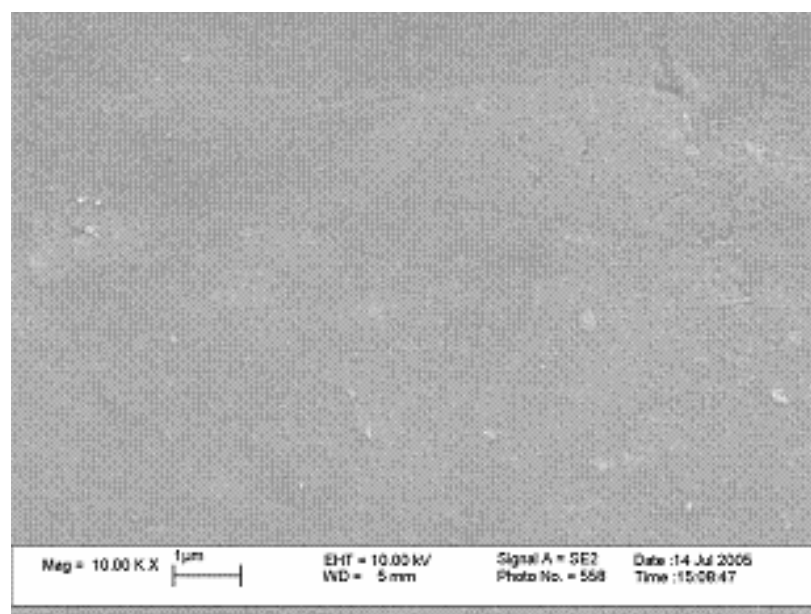


Figure 4-10: SEM of crosslinked PPP membrane (10K)

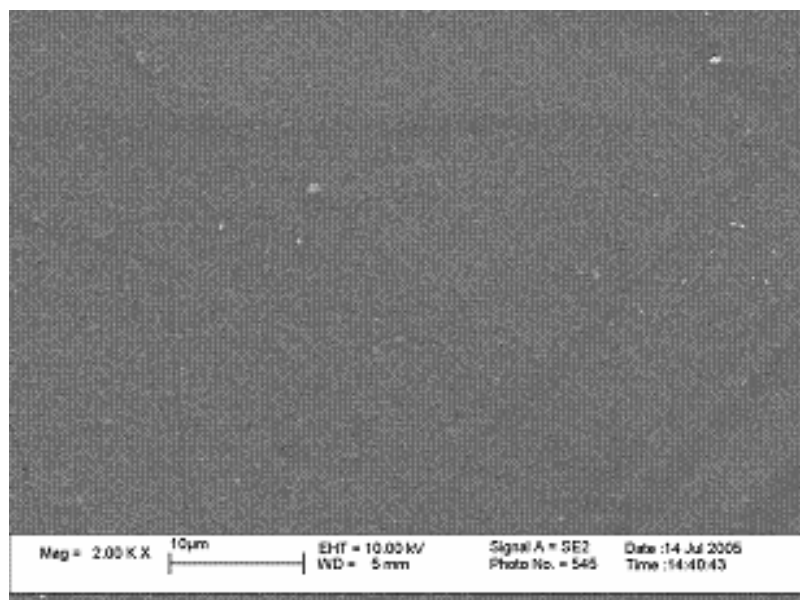


Figure 4-11: SEM of crosslinked PPS membrane (2K)

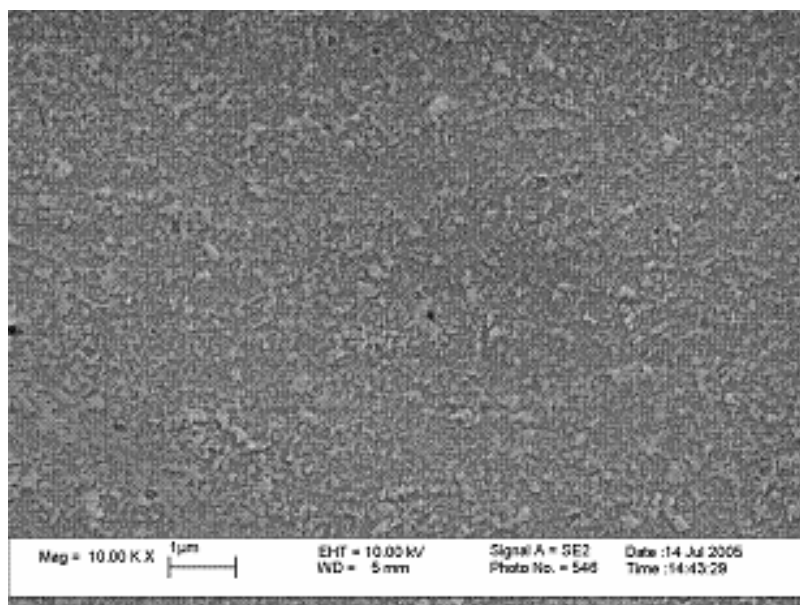


Figure 4-12: SEM of crosslinked PPS membrane (10K)

Table 4-4: Ionic conductivity results in Method I

Sample	Temperature	Ionic Conductivity (S/cm)
PEM in method I	Room Temperature	1.2 E-02
	80°C	2.8 E-02

Ionic Conductivity

The ionic conductivity for the membrane with a 4-point fixture immersed in water was measured. The results shown in Table 4-4 are: 1.2 E-02 S/cm at room temperature, and 2.8 E-02 S/cm at 80 °C.

4.4.2 Method II – PCS

FT-IR

A. Crosslinked PCHD membrane (sample 188-I):

Figure 4-13 shows the IR result of crosslinked PCHD membrane, in which the peak between 2990 and 2850 in X-axis was caused by the -CH₂- group.

B. After Sulfonation

Figure 4-14 shows the different IR result after the reaction of sulfonation. The strong peaks in 1250-1150, and 1060-1030 are caused by the groups of -SO₃H and S=O (S=O stretch), respectively.

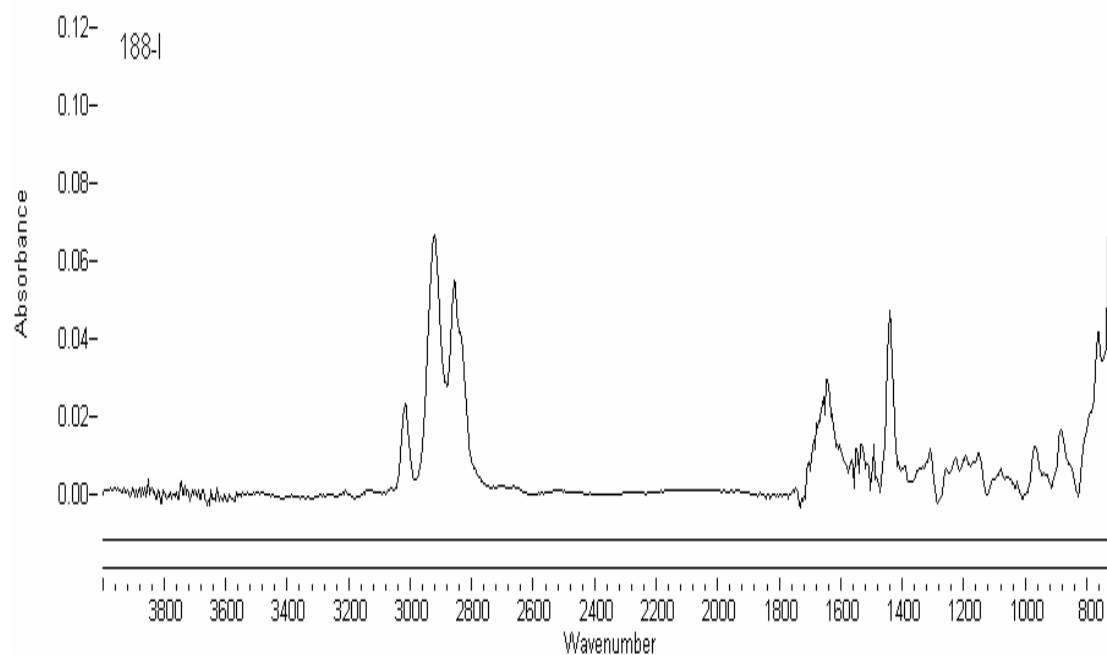


Figure 4-13: IR of crosslinked PCHD membrane

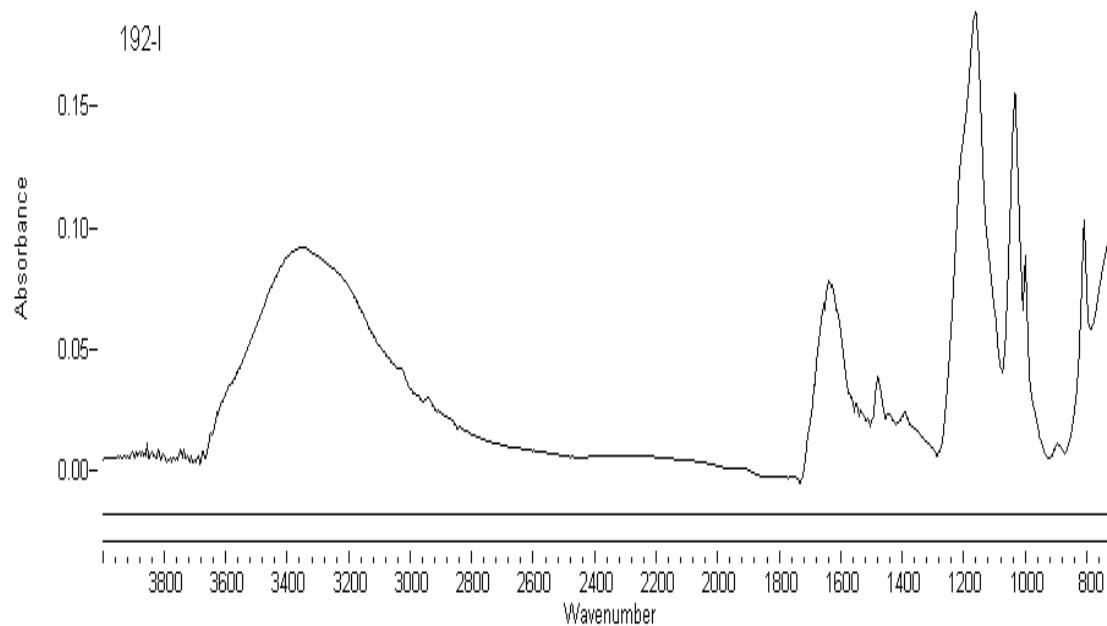


Figure 4-14: IR of crosslinked PCHD membrane after sulfonation

TGA

The TGA of membrane before sulfonation was expressed by the solid line of “1” in Figure 4-15. TGA of membrane after sulfonation was pretreated up to 150 °C, to get rid of water absorbed on the sulfonated membrane surface. When the membrane after sulfonation cooled down to room temperature, it was then measured on TGA up to 200 °C (shown in the dash line of “2”). We can see that the thermal stability of membrane after sulfonation is improved.

Elemental analysis

From the molar ratio of carbon/sulfur obtained from elemental analysis shown as in Table 4-5, the degree of sulfonation in Method II was also calculated by the formula: the sulfonation extent = [(Sulfur/C₆ after sulfonation) – (Sulfur/C₆ before sulfonation)] *

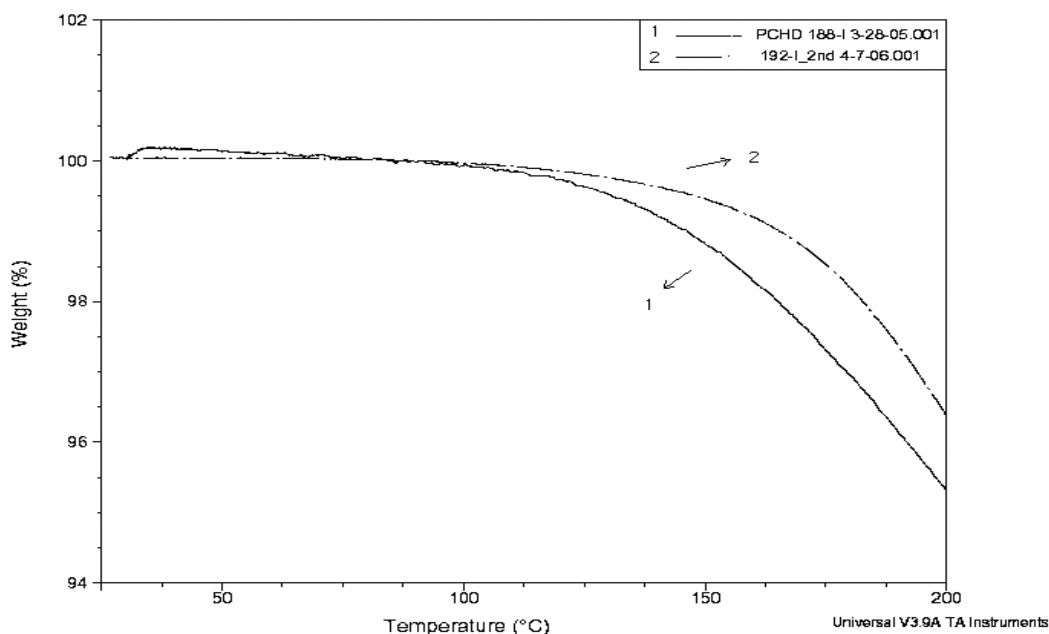


Figure 4-15: TGA results in Method II

Table 4-5: Elemental analysis in Method II

Sample ID	Analysis	Results
Sample 188-I (after crosslinking, but before sulfonation)	Carbon%	81.1%
	Sulfur%	5.2%
	Sulfur/C ₆	0.15
Sample 192-I (after sulfonation)	Carbon%	50.43%
	Sulfur%	10.47%
	Sulfur/C ₆	0.47

100%. The sulfonation degree here is 32.2%.. It is obvious that the sulfonation degree in Method II is more than Method I

Water-uptake

Table 4-6 showed the ability of absorbing water in membranes after sulfonation. We can obtain that the ability of absorbing water is better after sulfonation, which was caused by the group of sulfonic acid – SO₃H.

SEM

To measure the structure of membrane surface, the analysis of SEM was carried out. The surface structure of membrane after the sulfonation reaction was also shown in the Figure 4-16 and Figure 4-17. Figure 4-16 showed the surface in the magnification of 1:2000, and Figure 4-17 was in 1:10000.

Table 4-6: Water-uptake results in Method II

Sample ID	Weight (before in boiling water)	Weight (after in boiling water)	Weight increase %
Sample 192-I (after sulfonation)	0.026 g	0.027 g	4.0%

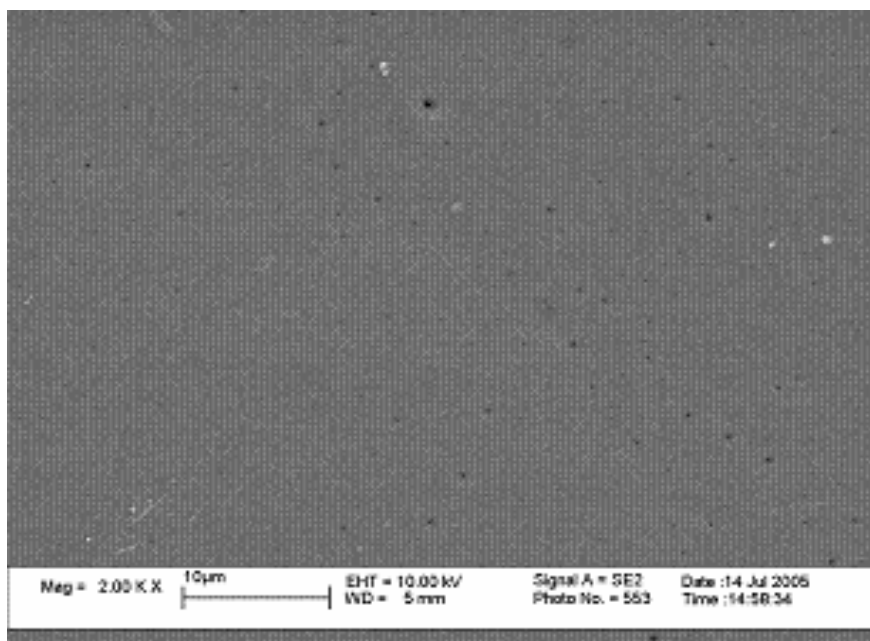


Figure 4-16: SEM of crosslinked PCHD membrane after sulfonation (2K)

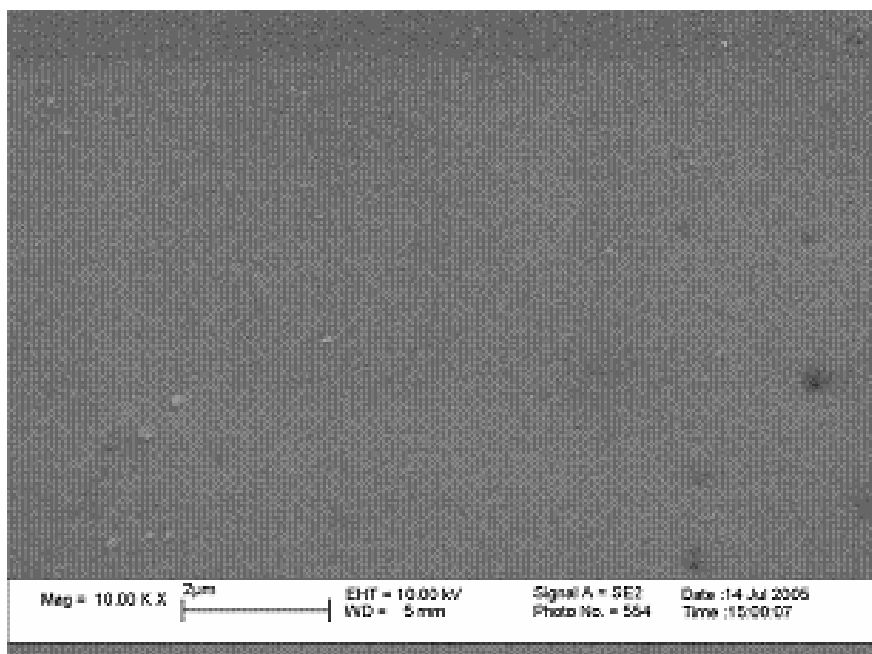


Figure 4-17: SEM of crosslinked PCHD membrane after sulfonation (10K)

Ionic Conductivity

The ionic conductivity for the membrane with a 4-point fixture immersed in water was measured and the results were shown in Table 4-7. The ionic conductivity is 1.6×10^{-2} S/cm in room temperature, and 3.6×10^{-2} S/cm at 80 °C. It is obvious that the ionic conductivity in Method II is better than in Method I. Although the results for the membrane in Method II is not good enough for the use in practice yet, we can do some further efforts in improving the ionic conductivity of membranes, such as increasing the ratio of acetic anhydride to sulfuric acid or using anhydrous acetic anhydride for higher degree of sulfonation.

Table 4-7: Ionic conductivity results in Method II

Sample	Temperature	Ionic Conductivity (S/cm)
PEM in method II	Room Temperature	1.6 E-02
	80°C	3.6 E-02

4.4.3 Method III – PASC

TGA

TGA results of Figure 4-18 explain the difference in the various membranes. The dash line and solid line represent the TGA results before and after the procedure of heat-press, respectively. It is obvious that after the heat-pressing, thermal stability of the membrane is much better than its precursor.

Elemental Analysis

From the results of elemental analysis shown in Table 4-8, the sulfur/phenyl is equal to the molar ratio between sulfonic acid group and phenyl group, and then the sulfonation degree was calculated to 32.4% by the formula: the sulfonation extent = (Sulfur/Phenyl)*100%.

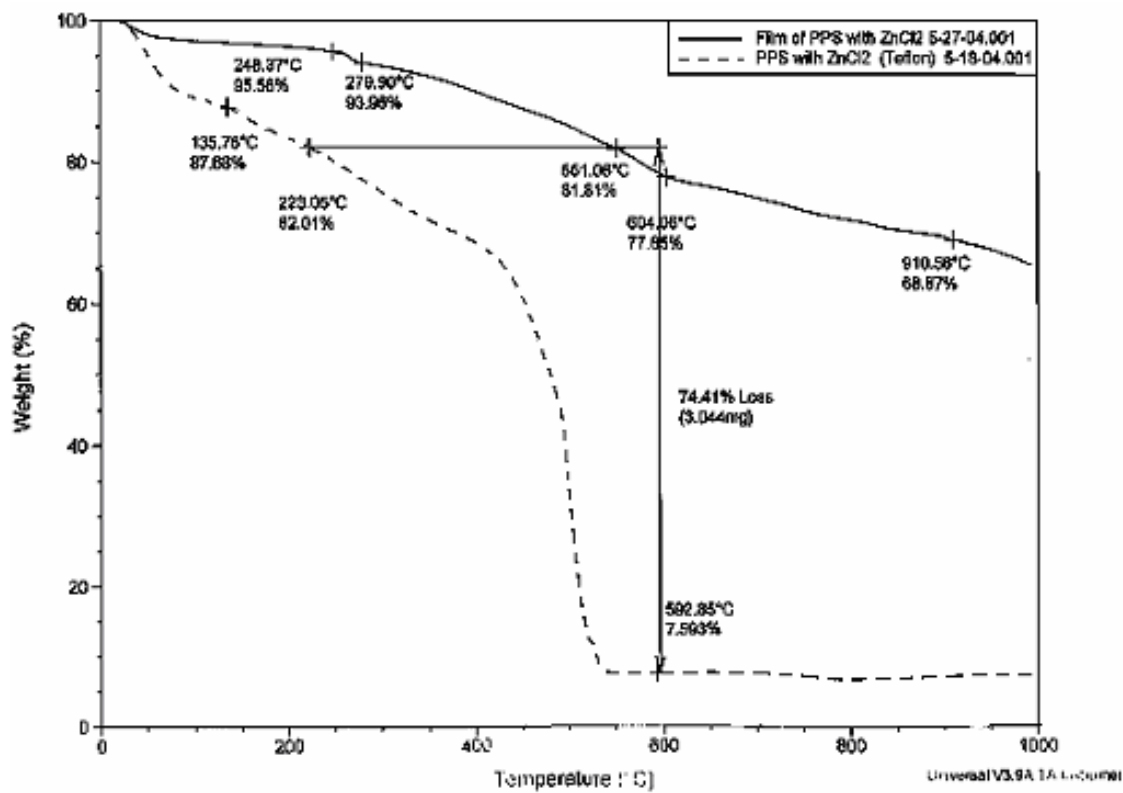


Figure 4-18: TGA results in Method III

Table 4-8: Elemental Analysis in Method III

	Carbon %	Sulfur %	Sulfur/Phenyl
PPS	51.9 %	7.5 %	0.32

4.5 Conclusions

4.5.1 Method I – PCAS

In Method I, sulfonated PEM based on PCHD was obtained, and the sulfonated PEM in decent size shows good thermal stability at relatively high temperature after aromatization. However, the ionic conductivity of PEM in Method I is not as good as in Method II.

4.5.2 Method II – PCS

In method II, another sulfonated PEM which did not experience the aromatization was obtained. Sulfonated PEM with decent size in Method II shows higher degree of sulfonation than in Method I.

4.5.3 Method III – PASC

In Method III, a PEM was obtained by heat-pressing at relatively high temperature. The sulfonation degree of PEM is high, and good thermal stability was observed after the process of heat-pressing. However, PEM is very brittle, and was not used practically as in Method I and method II.

CHAPTER 5

CONCLUSIONS

5.1 Summary

Hydrogen pipeline

In hydrogen pipeline research, PET/clay nanocomposite and sulfonated PET/clay nanocomposite were produced. TEM and SAXS were used to measure the exfoliation level of nanocomposites. TGA was used to see what effect on thermal stability the sulfonation and the mixing with clay could cause. Mixing PET with clay increased the hydrogen barrier properties. The hydrogen permeability of S-PET with clay should be measured in future work.

PEMs in fuel cells

Our research objective with PEM materials was to synthesize novel polymer electrolyte membranes based on poly(1,3-cyclohexadiene) (PCHD) with outstanding potential for use in hydrogen methanol fuel cells at temperatures well above 100 °C. Ideally, it could be less expensive and thermally stable at relatively high temperature (100+ °C). After the consecutive crosslinking, aromatization and sulfonation reactions, or the consecutive crosslinking and sulfonation reactions, some novel PEM materials based on PCHD were synthesized and characterized by FT-IR to verify the reaction of sulfonation. Elemental analysis was used to measure the extent of sulfonation, and to determine the optimistic method of sulfonation from several different ways. The good thermal stability was

measured by TGA and differential scanning (DSC) are measured. Scanning electron microscopy (SEM) was also carried out to determine the surface morphology of PEM materials based on PCHD. Water sorption was also calculated after the PEMs were soaked in distilled water, and the sulfonated group could also be further verified by this way. Thinner PEM membranes less than 0.2 mm need to be synthesized.

5.2 Future Work

Hydrogen pipeline

We sulfonated PET in order to create partially sulfonated PET. This material is expected to facilitate the formation of highly exfoliated structures because of specific electrostatic interactions between PET/-SO₃Na and clay particle surface. These strong interactions could make the clays more easily aligned with polymer chains and will create much better barrier materials. The hydrogen permeability evaluation of S-PET/clay nanocomposites is in progress. But the brittleness of S-PET due to low molecular weight could hold back the application of these nanocomposites. To solve this problem, we are synthesizing high molecular weight sulfonated PET, and modifying the mixing procedure to make S-PET/clay nanocomposites.

We are starting to optimize processing via melt-mixing in extruder. High levels of exfoliation in PET/clay and S-PET/clay nanocomposites, coupled with higher clay loadings, will result in enhanced hydrogen barrier properties for these materials. In addition, the creation of these nanocomposites using extruder mixing without using solvents will be explored as a more viable processing strategy.

PEM in fuel cells

The bigger reactor with the diameter over 15 inches was made to produce bigger PEMs.

Some further efforts are needed to improve the ionic conductivity of PEM both in Method I and Method II. For example, thinner membranes should be made in the future to improve ionic conductivity, the ratio of acetic anhydride to sulfuric acid or the reaction temperature can also be increased to increase the sulfonation degree, then to improve the ability of ionic conductivity.

LIST OF REFERENCE

1. M. Conte, A.I., M. Ronchetti, R. Vellone, *Hydrogen economy for a sustainable development: state-of-the-art and technological perspectives*. Journal of Power Sources, 2001. **100**: p. 171-187.
2. Penner, S.S., *Steps toward the hydrogen economy*. Energy, 2006. **31**: p. 33-43.
3. Dunn, S., *Hydrogen futures: toward a sustainable energy system*. International Journal of Hydrogen Energy, 2002. **27**: p. 235-264.
4. *DOE Hydrogen Program*. 2004, U.S. Department of Energy.
5. George W. Carbtree, M.S.D., and Michelle V. Buchanan, *The Hydrogen Economy*. Physics Today, 2004: p. 39-44.
6. *Hydrogen status and possibility*. 2002.
7. Farrauto, R.J., *Introduction to solid polymer membrane fuel cells and reforming natural gas for production of hydrogen*. Applied Catalysis B: Enviromental, 2005. **56**: p. 3-7.
8. *Hydrogen Posture Plan*, U.S.D.o. Energy, Editor. 2004.
9. *A National Vision of America's Transition To A Hydrogen Economy -- To 2030 And Beyond*, U.S.D.o. Energy, Editor. 2002.
10. Rostrup-Nielsen, T., *Manufacture of hydrogen*. Catalysis Today, 2005. **106**: p. 293-296.
11. Bjørnar Kruse, S.G., Cato Buch (2002) *Hydrogen - Status and possibilities*. Bellona Report **Volume**,
12. *National Hydrogen Energy Roadmap*, U.S.D.o. Energy, Editor. 2002.
13. Gunnar Birgisson Esq., W.L.E., *An effective regulatory regime for transportation of hydrogen*. International Journal of Hydrogen Energy, 2004. **29**: p. 771-780.

14. K. K. Chawla, J.M.R., J. B. Woodhouse, *Hydrogen-induced cracking in two linepipe steels*. Journal of Materials Science, 1986. **21**: p. 3777-3782.
15. M. Y. B. Zakaria, T.J.D., *Stack cracking by hydrogen embrittlement in welded pipeline steel*. Journal of Materials Science, 1991. **26**: p. 2189-2194.
16. Thompson, A.W., *Selection of structural materials for hydrogen pipelines and storage vessels*. International Journal of Hydrogen Energy, 1977. **2**: p. 163-173.
17. EG&G Technical Services, I., Science Applications International Corporation, *Fuel Cell Handbook*. 2002.
18. Wald, M.L., *Questions about a Hydrogen Economy*. Scientific American, 2004. **290**(5).
19. Winter, C.-J., *Into the hydrogen energy economy -- milestones*. International Journal of Hydrogen Energy, 2005. **30**: p. 681-685.
20. Michael A. Hickner, H.G., Yu Seung Kim, *Alternative Polymer Systems for Proton Exchange Membranes (PEMs)*. Chem Rev., 2004. **104**: p. 4587-4612.
21. Biyikoglu, A., *Review of proton exchange membrane fuel cell models*. International Journal of Hydrogen Energy, 2005. **30**: p. 1181-1212.
22. Dennis E. Curtin, R.D.L., Timothy J. Henry, Paul C. Tangeman, Monica E. Tisack, *Advanced materials for improved PEMFC performance and life*. Journal of Power Sources, 2004. **131**: p. 41-48.
23. Shoibal Banerjee, D.E.C., *Nafion perfluorinated membranes in fuel cells*. Journal of Fluorine Chemistry, 2004. **125**: p. 1211-1216.
24. B. Smitha, S.S., A.A. Khan, *Solid polymer electrolyte membranes for fuel cell applications -- a review*. Journal of Membrane Science, 2005. **259**: p. 10-26.

25. Yu Seung Kim, L.D., Michael A. Hickner, Thomas E. Glass, Vernon Webb, and James E. McGrath, *State of water in disulfonated poly(arylene ether sulfone) copolymers and a perfluorosulfonic acid copolymer (Nafion) and its effect on physical and electrochemical properties*. Macromolecules, 2003. **36**(17): p. 6281-6285.
26. Minh, N.Q., *Solid oxide fuel cell technology -- features and applications*. Solid State Ionics, 2004. **174**: p. 271-277.
27. Mark A.J. Cropper, S.G., David M. Jollie, *Fuel cells: a survey of current developments*. Journal of Power Sources, 2004. **131**: p. 57-61.
28. Bruijin, F.d., *The current status of fuel cell technology for mobile and stationary applications*. Green Chem., 2005. **7**: p. 132-150.
29. Mark C. Williams, J.P.S., Wayne A. Surdoval, *The U.S. department of energy, office, of fossil energy stationary fuel cell program*. Journal of Power Sources, 2005. **143**: p. 191-196.
30. Cropper, M., *Fuel cells for people*, in *Fuel Cell Today*. 2004: London.
31. Guozhen Zheng, T.S., Katsuhiko Takagi, *PET-clay hybrids with improved tensile strength*. Materials Letters, 2003. **57**: p. 1858-1862.
32. Chun-cheng Li, D.Z., Zhen-yi Li, *Synthesis and properties of poly(ester ether) multiblock copolymers/organomontmorillonite hybrid nanocomposite*. Journal of Applied Polymer Science, 2002. **84**: p. 1716-1720.
33. Beyer, G. (Oct 2002) *Nanocomposites: a new class of flame retardants for polymers*. Plastics Additives & Compounding **Volume**, 22-28

34. O. Gain, E.E., *Gas Barrier Properties of Poly(ϵ -caprolactone)/Clay Nanocomposites: Influence of the Morphology and Polymer/Clay Interactions* Journal of Polymer Science: Part B: Polymer Physics, 2005. **43**: p. 205-214.
35. Alexander B. Morgan, J.D.H., *Exfoliated polystyrene-clay nanocomposites synthesized by solvent blending with sonication*. Polymer, 2004. **45**: p. 8695-8703.
36. T.D. Fornes, D.R.P., *Structure and properties of nanocomposites based on Nylon-11 and -12 compared with those based on Nylon-6*. Macromolecules, 2004. **37**: p. 7698-7709.
37. Frederick L. Beyer, N.C.B.T., Arnab Dasgupta, and Mary E. Galvin, *Polymer-layered silicate nanocomposites from model surfactants*. Chem. Mater., 2002. **14**: p. 2983-2988.
38. Kazuhisa Yano, A.U., Akane Okada, Toshio Kurauchi, Osami Kamigaito, *Synthesis and properties of polyimide-clay hybrid*. Journal of Polymer Science Part A: Polymer Chemistry, 2003. **31**(10): p. 2493-2498.
39. Sang-Soo Lee, Y.T.M., hee-Woo Rhee, Junkyung Kim, *Exfoliation of layered silicate facilitated bby ring-opening reaction of cyclic oligomers in PET-clay nanocomposites*. Polymer, 2005. **46**: p. 2201-2210.
40. Grant D. Barber, B.H.C., Robert B. Moore, *Poly(ethylene terephthalate) ionomer based clay nanocomposites produced via melt extrusion*. Polymer, 2005. **46**: p. 6706-6714.
41. Guozhen Zhang, T.S., Katsuhiko Takagi *PET-clay hybrids with improved tensile strength*. Materials Letters, 2003. **57**: p. 1858-1862.

42. Ou CF, H.M., Lin JR, *Synthesis and characterization of poly(ethylene terephthalate) nanocomposites with organoclay*. Journal of Applied Polymer Science, 2004. **91**(1): p. 140-145.
43. Alexander A. Lambert III, K.A.M., David A. Schiraldi, *[Poly(ethylene terephthalate) ionomer]/silicate hybrid materials via polymer-in situ sol-gel reactions*. Journal of Applied Polymer Science, 2002. **84**: p. 1749-1761.
44. Bret J. Chrisholm, R.B.M., Grant Barber, *Nanocomposites derived from sulfonated poly(butylene terephthalate)*. Macromolecules, 2002. **35**: p. 5508-5516.
45. Page KA, S.G., Moore RB, *Influence of ionic aggregation on the surface energies of crystallites in poly(butylene terephthalate) ionomers*. Polymer, 2004. **45**(25): p. 8425-8434.
46. B. Smitha, S.S., A.A. Khan, *Synthesis and characterization of proton conducting polymer membranes for fuel cells*. Journal of Membrane Science, 2003. **225**: p. 63-76.
47. Akira Yamauchi, K.T., Ashraf M. Chaudry, A. Mounir EL Sayed, *Characterization of charged film of fluorocarbon polymer (Nafion) and blended fluorocarbon polymer (Nafion)/Collodion composite membranes by electrochemical methods in the presence of redox substances. V*. Journal of Membrane Science, 2005. **249**: p. 119-126.
48. Guojun Liu, X.Y., *Preparation and static light-scattering study of polystyrene-block-polyisoprene nanofiber fractions*. . Macromolecules, 2002. **35**(26): p. 9788-9793.

49. Hong, K.M., Jimmy; Wang, Yuming; Advincula, Rigoberto., *Synthesis and aromatization of polycyclohexadiene (PCHD) homo- and block co-polymers: towards processable poly-p-phenylene (PPP) derivatives.* . Polymeric Materials Science and Engineering, 1999. **80**: p. 116-117.
50. Marvel, C.S.H., Gordon E., *Preparation and aromatization of poly-1,3-cyclohexadiene.* . Journal of the American Chemical Society, 1959. **81**: p. 448-452.
51. Baigl, D.S., Thomas A. P.; Williams, Claudine E., *Preparation and Characterization of Hydrosoluble, Partially Charged Poly(styrenesulfonate)s of Various Controlled Charge Fractions and Chain Lengths.* Macromolecules, 2002. **35**(6): p. 2318-2326.
52. Carretta, N.T., V.; Picchioni, F., *Ionomeric membranes based on partially sulfonated poly(styrene): synthesis, proton conduction and methanol permeation.* . Journal of Membrane Science, 2000. **166**(2): p. 189-197.
53. Kunlun Hong, J.W.M., *1,3-Cyclohexadiene Polymers. I. Anionic Polymerization.* Macromolecules, 2001. **34**: p. 782-786.
54. Xing Fu Zhong, B.F., *Kinetics of 1,3-cyclohexadiene polymerization initiated by organolithium compounds in a non-polar medium, I pure propagation step.* Makromol. Chem, 1990. **191**: p. 2735-2741.
55. Williamson, D.T.E., James F.; Madison, Phillip H.; Pasquale, Anthony J.; Long, Timothy E., *Synthesis and Characterization of Poly(1,3-cyclohexadiene) Homopolymers and Star-Shaped Polymers.* Macromolecules, 2001. **34**(7): p. 2108-2114.

56. Imaizumi, K.O., Takashi; Natori, Itaru; Sakurai, Shinichi; Takeda, Kunihiro., *Microphase-separated structure of 1,3-cyclohexadiene/butadiene triblock copolymers and its effect on mechanical and thermal properties.* . Journal of Polymer Science, Part B: Polymer Physics, 2001. **39**(1): p. 13-22.
57. Natori, I.I., Kimio; Yamagishi, Hideyuki; Kazunori, Miyuki., *Hydrogen polymers containing six-membered rings in the main chain. Microstructure and properties of poly(1,3-cyclohexadiene).* Journal of Polymer Science, Part B: Polymer Physics, 1998. **36**(10): p. 1657-1668.
58. Vallejo, E.P., Gerald; Gavach, Claude; Mercier, Regis; Pineri, Michel. , *Sulfonated polyimides as proton conductor exchange membranes. Physicochemical properties and separation H^+/Mz^+ by electrodialysis comparison with a perfluorosulfonic membrane.* . Journal of Membrane Science 1999. **160**(1): p. 127-137.
59. Miyatake, K.F., Kazuaki; Takeoka, Shinji; Tsuchida, Eishun., *Nonaqueous Proton Conduction in Poly(thiophenylenesulfonic acid)/Poly(oxyethylene) Composite.* . Chemistry of Materials, 1999. **11**(5): p. 1171-1173.
60. Miyatake, K.S., Eiichi; Yamamoto, Kimihisa; Tsuchida, Eishun., *Synthesis and proton conductivity of highly sulfonated poly(thiophenylene).* . Macromolecules, 1997. **30**(10): p. 2941-2946.
61. Koji Ishizu, A.O., *Core-Shell Type Polymer Microspheres Prepared by Domain Fixing of Block Copolymer Films.* Journal of Polymer Science: Part A: Polymer Chemistry, 1989. **27**: p. 3721-3731.

62. Glazer, J.a.J.H.S., *Vulcanization of crepe rubber by sulfur monochloride. Part I. The gelation method.* . Journal of Polymer Science, 1954. **14**: p. 169-179.
63. Xing Fu Zhong, B.F., *Soluable polystyrene-block-poly(p-phenylene) block copolymers prepared from polystyrene-block-poly(1,3-cyclohexadiene) precursors. Study of the aromatization process.* Makromol. Chem., 1991. **192**: p. 2277-2291.
64. Ramamoorthy, M.R., Mohan Doraiswamy., *Cellulose Acetate and Sulfonated Polysulfone Blend Ultrafiltration Membranes. Part III. Application Studies.* . Industrial & Engineering Chemistry Research, 2001. **40**: p. 4815-4820.
65. Kwon, H.R.A.a.S., *An ionically cross-linkable polyphosphazene: Poly[bis(carboxylatophenoxy)phosphazene] and its hydrogels and membranes.* Macromolecules, 1989. **22**(1): p. 75-79.

VITA

Hongliang Zhou was born in Wuwei, Anhui province on April 24, 1979. He went to high school at Wuwei The First High School in the same city. In 2001, He graduated from East China University of Science and Technology with a Bachelor Engineering degree in the city of Shanghai after the four years of undergraduate study. In Sep 2001, he was admitted into the Chemistry Department, East China University of Science and Technology in Shanghai for graduate study and obtained the Master Science degree.

In Aug 2003, he came to University of Tennessee, Knoxville (UTK), Department of Chemistry, and joined Professor Jimmy W. Mays's group for the graduate study, earning the degree of Master of Science in Polymer Chemistry in May 2006.